

## **PROGRESS REPORT (Quarterly)**

### **1. DOE Award Number and Name of Recipient**

Award number: DE-NT0005287

Name of recipients: Georgia Tech Research Corporation

### **2. Project Title and Name of Project Director/PI**

Title: Reversible Ionic Liquids as Double-Action Solvents for Efficient CO<sub>2</sub> Capture

PI: Dr. Charles. A. Eckert

Co-PI: Dr. Charles L. Liotta

### **3. Date of Report and Period Covered**

Date of report: October 31, 2010

Period covered: July 1, 2010 – September 30, 2010 (Budget Period 2 – Q4)

### **4. Executive Summary**

The objective of this project is to develop reversible ionic liquids as solvents for post-combustion recovery of CO<sub>2</sub> from fossil fuel-fired power plants. These novel solvents are neutral molecules which react with CO<sub>2</sub> to form an ionic liquid, which then dissolves additional CO<sub>2</sub> by a physisorption mechanism. Subsequently, modest elevations in temperature reverse the reaction and yield pure CO<sub>2</sub> for sequestration. Because of this dual-mode capture ability, capacity can be large, and we are modifying the precursor structure using structure-property relationships to optimize both physical and thermodynamic properties. By incorporating silanes

in the molecules we reduce viscosity, thereby improving the mass transfer rates of CO<sub>2</sub> absorption/desorption and decreasing the processing costs for pumping the solvent.

We are designing, testing, and optimizing reversible ionic liquids for application to CO<sub>2</sub> capture and we shall do the process design and cost analysis for their implementation. In addition, we shall develop a process for commodity-scale production of our solvents.

We continue to make substantial progress throughout the second year of this project, meeting or exceeding projected achievements. Our major contributions through the eighth quarter include:

- We have completed characterization for both the molecular and ionic liquid forms of (3-aminopropyl) diisopropyl(1H,1H,2H,2H-perfluoropentyl) silane. Two new compounds (3-aminopropyl) cyclohexyldimethyl silane and (3-aminopropyl) phenyldimethyl silane were also synthesized and preliminary characterization was done on the former. ***With this we have successfully synthesized eight silyl-amine compounds (molecular precursors) for dual-mode CO<sub>2</sub> capture. (TASK 2 and TASK 5)***
- We have analyzed the effects of the size of the substituent groups on both the ***thermodynamics and the CO<sub>2</sub> capture capacities*** by comparing three alkyl-substituted silanes: (3-aminopropyl) triethylsilane, (3-aminopropyl) tripropylsilane, and (3-aminopropyl) trihexylsilane. ***(TASK 4 and TASK 5)***
- We have also completed the FT-IR calculations examining the ***physical absorption and Henry's Law constants*** of CO<sub>2</sub> in the 6 silyl-amine based RevILs: (3-aminopropyl) trimethoxysilane, (3-aminopropyl) triethoxysilane, (3-aminopropyl) triethylsilane, (3-aminopropyl) tripropylsilane, (3-aminopropyl) trihexylsilane and (3-aminopropyl) diisopropyl (1H,1H,2H,2H-perfluoropentyl)silane. Operating pressures up to 60 bar and

temperatures of 35°C and 50°C were examined using attenuated total reflectance (ATR) Fourier transform infrared (FT-IR) spectroscopy and our Generation 3 custom made high pressure reaction vessel. **(TASK 4 and TASK 5)**

- The density data for the 6 silyl-amine RevILs has been completed for both molecular and ionic liquids as a function of temperature. **(TASK 4)**
- Preliminary correlations between viscosity, refractive index, and extent of conversion have been established. **(TASK 5)**

Our goal remains to minimize the cost and energy requirements of CO<sub>2</sub> capture to help DOE meet its goal – 90% CO<sub>2</sub> capture with no more than a 30% increase in cost by 2020.

## 5. Results of Work

### a. Approach

#### *I-* Synthesis and Characterization of Custom Reversible ILs

We proposed to investigate the use of a variety of basic nitrogen containing compounds such as amines and guanidines based materials for the capture and subsequent controlled release of CO<sub>2</sub>. The reaction scheme for the synthesis of silyl-amine based molecular solvent is shown (Figure 1).

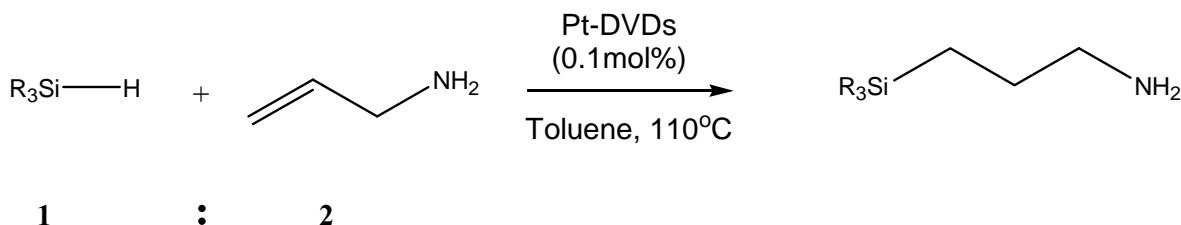


**Figure 1. One-step synthetic scheme for silyl-amine based RevILs.**

The synthetic scheme being employed affords two main benefits for the production of RevILs for CO<sub>2</sub> capture from flue gas: (1) the synthesis is simple and efficient and (2) the structure can be easily modified by simply changing the substitution on the starting silane. This allows for the development of a plethora of compounds to be tested for application to CO<sub>2</sub> capture, as well as ensuring that the optimal candidate will be capable of scaling to synthesis on an industrial level. Additionally, as progress is made on existing compounds, we can identify molecular structures for improved absorption capacities and processing properties and alter the current synthetic techniques by simple substitution of silanes. *With progressive improvements to the molecular structure we aim to develop an optimal CO<sub>2</sub> capture solvent with a decrease in the operating costs (relative to monoethanolamine absorption).*

After synthesis and isolation, each compound was thoroughly characterized via <sup>1</sup>H, <sup>13</sup>C NMR, Elemental analysis, FT-IR, and DSC/TGA thermograms. Then, each molecular liquid was reacted with CO<sub>2</sub> to produce an ionic liquid capable of further physi-sorption (Figure 2). The resulting ionic species (liquid or solid) was characterized by <sup>1</sup>H and <sup>13</sup>C NMR, melting point (if applicable), DSC, FT-IR, and solvatochromatic measurements.

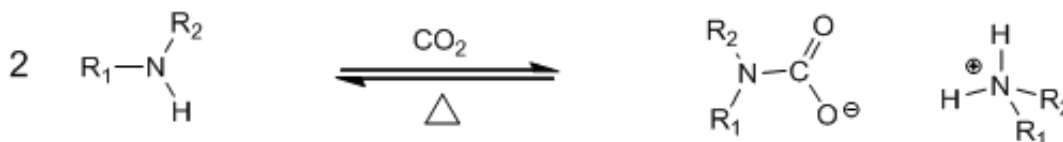


**Figure 2. Reaction of custom-made amine with CO<sub>2</sub> to form reversible ionic liquids.**

The solvatochromic polarity measurements will be performed using an HP 8453 UV-Vis Spectrophotometer and the polarity probe Nile Red. The wavelength of maximum absorption ( $\lambda_{max}$ ) for the probe in a given solvent is a good measure of the polarity of the solvent. The  $\lambda_{max}$  of Nile Red has been found and reported for hundreds of solvents, making this an efficient approach for determination of solvent polarity.

The loss of CO<sub>2</sub> upon heating and thermal stability of the amines is explored using NMR and differential scanning calorimetry (DSC). The DSC experiments are performed on a Q20 TA Instruments machine, with a temperature profile of 5°C/min from an initial temperature of -40°C to a final temperature of 400°C. The first endotherm was taken to represent the loss of CO<sub>2</sub> with the second endotherm representing the vaporization of the molecular liquid.

Although stability tests confirmed that the trialkyl-substituted precursors were stable over a period of two months in both water- and oxygen-containing environments, we shall still perform the experiment on the precursors that show promising thermodynamic properties or absorption capacities to ensure industrial viability of our new solvents. Stability will be monitored using <sup>1</sup>H NMR.

## **2- Thermodynamics of CO<sub>2</sub> Capture**

Thermodynamics of these systems is summed up by three main quantities of interest: the equilibrium constant  $K(T)$ , the difference between the reversion temperature and CO<sub>2</sub> capture temperature  $\Delta T = T_{rev} - T_{fwd}$ , and the enthalpy required for regeneration of silyl-amine from the ionic liquid  $\Delta H_{regeneration}$ . These quantities are highly interrelated to each other. The equilibrium constant  $K(T)$  determines the equilibrium conversion of the molecular precursor (silyl-amine) at a given temperature and is independent of CO<sub>2</sub> pressure. A favorable silyl-amine will have a high

K ( $K > 1$ ) at the CO<sub>2</sub> capture temperature ( $T_{\text{fwd}}$ ) to ensure maximum conversion of the molecular precursor to the ionic liquid, and a low K value ( $K < 1$ ) at the reversion temperature ( $T_{\text{rev}}$ ) to ensure complete regeneration of the silyl-amine. These K values are also related to the reaction enthalpies by

$$\frac{d \ln K(T)}{d T} = \frac{\Delta H_{\text{rxn}}}{RT^2} \quad (1)$$

where  $\Delta H_{\text{rxn}}$  is the enthalpy of reaction between the molecular liquid and CO<sub>2</sub> to give ionic liquid (and vice versa). The above equation implies that if the K values are extremely high ( $K \gg 1$ ) or extremely low ( $K \ll 1$ ),  $\Delta H_{\text{rxn}}$  will be large leading to huge energy penalty ( $\Delta H_{\text{regeneration}}$ ) for regeneration of the silyl-amine.

The second quantity of interest is  $\Delta T = T_{\text{rev}} - T_{\text{fwd}}$ , where  $T_{\text{fwd}}$  is the temperature at which CO<sub>2</sub> is captured and  $T_{\text{rev}}$  is the reversal temperature. This quantity determines the heat input required to raise the temperature of the ionic liquid to the  $T_{\text{rev}}$ ,

$$Q = m C_p \Delta T \quad (2)$$

$m$  is the mass of the ionic liquid and  $C_p$  is the heat capacity. In the actual absorber unit,  $T_{\text{fwd}}$  will be dictated by the temperature of flue gas stream, hence we will choose  $T_{\text{fwd}}$  as a basis temperature (say 40°C) for all our compounds. The quantity that will change with the choice of molecular liquid will be  $T_{\text{rev}}$ . To minimize the heat input for heating the ionic liquid, we would prefer lower values of  $T_{\text{rev}}$ , however Equation (1) also implies that small values of  $\Delta T$  (hence  $T_{\text{rev}}$ ) will lead to large reaction enthalpies for regeneration. Therefore, we are looking for compounds that give optimum values of  $T_{\text{rev}}$ .

Since our compounds capture CO<sub>2</sub> through dual mode, two kinds of enthalpies constitute the enthalpy required for regeneration of the molecular liquid:  $\Delta H_{\text{regeneration}} = \Delta H_{\text{rxn}} + \Delta H_{\text{dissolution}}$ .  $\Delta H_{\text{rxn}}$  is associated with removing the chemisorbed CO<sub>2</sub> and  $\Delta H_{\text{dissolution}}$  with the physisorbed CO<sub>2</sub>.

In the following discussion we will elaborate on the experimental techniques that we have employed for calculating the three quantities discussed above. The equilibrium constant,  $K(T)$ , representative of the capture (and release) of CO<sub>2</sub> can be found by measuring the equilibrium concentrations of reactants (the precursor molecule and CO<sub>2</sub>), and the product (ionic liquid) at a given temperature, and then correcting for the nonideal behavior of these species.

$$K(T) = \frac{\gamma_{IL}x_{IL}}{(\gamma_{ML}x_{ML})^2\gamma_{CO_2}x_{CO_2}} \quad (3)$$

where  $x_i$  are the mole fraction of the species and  $\gamma_i$  the activity coefficients. In evaluating  $K(T)$ , we are going to use the conversion of the molecular liquid to ionic liquid as well as the dissolved CO<sub>2</sub> concentration as measured by the FT-IR. We shall evaluate the equilibrium constant with an activity based approach to account for the nonideality of the mixture. We expect the system to exhibit a nonideal behavior because of the highly polar nature of the liquid phase and the dissimilarity of the molecules in the system (CO<sub>2</sub>, the amine precursor, and the highly polar and viscous ionic liquid).

We are using attenuated total reflectance (ATR) Fourier-transform infrared (FT-IR) spectroscopy to determine the conversion under a broad range of conditions. ***This measurement technique allows for the simultaneous measurement of chemical and physical absorption CO<sub>2</sub> capacity, both used for the determination of the thermodynamic properties of the solvent.*** The ATR FT-IR optics bench used for data collection will be the Heated Golden Gate ATR sample

accessory supplied by Specac, with a working temperature range up to 300°C and pressure rating for the tungsten carbide embedded diamond being 15,000psi.

The evaluation of the equilibrium constant involves the estimation of the activity coefficient ( $\gamma$ ) with excess Gibbs energy models. Conventionally, these models contain one or more adjustable parameters that are optimized to best fit the experimental data. In ternary systems, the binary interaction parameters are first obtained from experimental Vapor-Liquid Equilibria (VLE) data for each pair of system components and are used to estimate the  $\gamma$  for ternary systems. However, since our reversible ionic liquids are synthesized in house (no previous experimental data available) and due to the nature of the system (the reversible ionic liquid is formed only in the presence of the molecular liquid and CO<sub>2</sub>), we are developing a unique approach to estimate the ternary system activity coefficients for the experimental data directly. We are currently reviewing published data and thermodynamic models for ionic liquids-CO<sub>2</sub>, organics-ionic liquids, electrolyte solutions, and ternary systems including variations of these components. We are considering various thermodynamic models that represent mixtures containing polar and non-polar components

In addition to examining thermodynamic models for computing  $\gamma$ , we are considering Raoult's law as a limiting case. Raoult's law assumes an ideal mixture with all  $\gamma$  values set at unity. This approach can be applied at the extremes – around minimal and around complete conversion of the ionic liquid – where the concentrations of two of the systems components are finite. We are gathering published data of infinite dilution activity coefficients for ionic liquids in organics and for organics in ionic liquids as well as Henry's constants for CO<sub>2</sub>. These values will be used as guidelines for the optimization of the equilibrium constants of our ionic liquids.

We had earlier discussed Differential Scanning Calorimetry (DSC) as a means for characterizing the CO<sub>2</sub> capture in our compounds. Here we have extended the applicability of this technique for calculation of  $\Delta H_{\text{regeneration}}$  and  $T_{\text{rev}}$ . As before, the preformed ionic liquid is heated in a DSC pan from -40°C to 400°C at a rate of 5C/min.  $\Delta H_{\text{regeneration}}$  is measured by calculating the total heat flow during the reversal, while  $T_{\text{rev}}$  is measured as the onset point of reversion event. Details of this are given in the discussion section.

### **3- CO<sub>2</sub> Capture Capacities**

Our principal objective in this project is to enhance the CO<sub>2</sub> capture capacities of our compounds through chemisorption and physisorption, without significantly increasing the process costs. The amount of CO<sub>2</sub> captured through chemisorption (reaction with the amine) is determined by the stoichiometry and the reaction temperature. All the silyl-amines discussed in this report contain single amine functionality, hence at complete conversion, two moles of these compounds react with a single mole of CO<sub>2</sub>. The physisorption, on the other hand, depends on the intermolecular void space in these silyl amines, their van der Waals attractions with CO<sub>2</sub>, and the partial pressure of the CO<sub>2</sub> gas stream in contact with the compound. We have systematically altered the structure of our compounds to enhance the physisorption capacities. In this quarter, we have extensively focused on determining the overall CO<sub>2</sub> capture capacity as well as the individual chemisorption and physisorption capacities.

We have employed gravimetric technique for determining the overall capture capacity of each compound. For these experiments, CO<sub>2</sub> at 1 bar was reacted with the molecular silyl-amines (silyl-amines) at room temperature. The overall capture capacity is determined by the net weight

gain after the completion of the reaction. This represents the combined chemisorption at maximum conversion and the physisorption at 1 bar of CO<sub>2</sub>.

Thermo-gravimetric Analysis (TGA) was conducted on the ionic liquids. The preformed ionic liquids were heated from room temperature to 400°C at a rate of 5°C/min and the weight loss was recorded using a TGA microbalance. We used the same heating profile for both the DSC and TGA to allow simultaneous analyses. The DSC thermograms clearly indicate two events: 1) the reversal of the ionic liquid to the molecular liquid (ionic liquid to silyl-amine and CO<sub>2</sub>) and 2) the silyl-amine vaporization. Using simultaneous analysis from DSC and TGA, we can attribute the weight loss associated with CO<sub>2</sub> removal and the silyl-amine vaporization. However, the ionic liquid sampled in our TGA is not in contact with 1 atm CO<sub>2</sub> but rather 1 atm air, thus lowering the amount of physically absorbed CO<sub>2</sub>. Therefore, the physical absorption capacity measured by this technique is lower than the gravimetric technique described earlier. It is also worth noting that the physisorption in the actual absorber will depend on the CO<sub>2</sub> partial pressure in the flue gas exhaust stream, which is lower than 1 atm but higher than the CO<sub>2</sub> partial pressure in the air.

Additionally, we reacted the molecular liquids with <sup>13</sup>C labeled CO<sub>2</sub> to differentiate and quantify the chemisorbed and physisorbed CO<sub>2</sub> present in the reversible ionic liquid. In parallel, we are using attenuated total reflectance (ATR) Fourier-transform infrared (FT-IR) spectroscopy to determine *simultaneous measurement of chemical and physical absorption CO<sub>2</sub> capacity*. Results from quantitative <sup>13</sup>C NMR experiments and FTIR experiment will be cross-examined.

The NMR used is a Bruker AMX 400 located in the School of Chemistry and Biochemistry at Georgia Tech. The ATR FT-IR optics bench used for data collection is the Heated Golden Gate ATR sample accessory supplied by Specac, with a working temperature

range up to 300°C and pressure rating for the tungsten carbide embedded diamond being 15,000psi. Equilibrium measurements are performed by using a custom-designed and -built ATR FT-IR high pressure reactor. Although the scrubbing will be carried out at our near atmospheric pressure, the pressure range of the instrument permits us to ascertain better the effect of CO<sub>2</sub> concentration on both equilibria and rates. Consultation for the design was offered by Prof. Sergei Kazarian of Imperial College London. We are now using a custom designed and built Generation 3 stainless steel reactor, which has been successfully tested at temperatures to 150°C and pressures to 1500psi.

We have performed two types of measurements using our FT-IR. In the first set, we placed the molecular precursor in the ATR cell and pressurized it with CO<sub>2</sub> at different temperature and pressure conditions. This allows us to make simultaneous measurements of concentration of molecular liquid, ionic liquid, and CO<sub>2</sub>. Data from these experiments will be presented in the subsequent quarterly progress reports. In the second set, we put the preformed ionic liquids in the ATR cell and measure the solubility of free CO<sub>2</sub> as a function of CO<sub>2</sub> pressure, and thus determine the Henry's law constants. The CO<sub>2</sub> that is in solution and not chemically bound to the amine (referred to as "free CO<sub>2</sub>") has a very distinct absorption band in the mid-infrared region (the  $\nu_3$  band of CO<sub>2</sub> at *ca.* 2335 cm<sup>-1</sup>). Following the Beer-Lambert Law, the absorbance of this band is directly proportional to the concentration of this "free CO<sub>2</sub>" absorbed in solution. A calibration curve relating the absorbance of CO<sub>2</sub> and the concentration was obtained for a methanol/CO<sub>2</sub> system using VLE data found in literature, to calculate the concentration of CO<sub>2</sub> at various temperatures and pressures. For the analysis, we also require density, refractive index, and molar absorptivity of the ionic liquid. Density measurements are conducted in our laboratory using an Anton Paar DMA 38 Laboratory Density Meter. Molar

absorptivities are calculated for the samples by examining the IR spectra of both the molecular and ionic liquids, and using the corresponding density and path length information. The simultaneous  $^1\text{H}$  NMR and FT-IR measurements were used to confirm this approach. The refractive index information, which will be used to calculate path length, is measured with an Arias 500 Refractometer. Changes in penetration depth will be accounted for by examining the refractive indices of the samples in both molecular and ionic forms. Density changes in the samples arising from conversion to ionic liquid and swelling of the liquid due to physical absorption is corrected by examining the C-H stretch vibrational frequencies ( $<3000\text{ cm}^{-1}$ ) in the samples.

#### **4- Other important Structure-Property relationships: Viscosity, Refractive index, and Density**

In the last report we presented the viscosities and refractive indices of six molecular and ionic liquids. One of the main challenges in the applicability of our solvents for  $\text{CO}_2$  capture is the high viscosities of the ionic liquids formed by  $\text{CO}_2$  absorption. However, our preliminary experiments showed that both the viscosity and the refractive indices are functions of conversion (extent of chemisorption) of the molecular precursor to the ionic form. In this report, we present some of our preliminary experiments that show the correlation between the viscosity, refractive index, and conversion. We are currently performing extensive studies where we simultaneously measure the different conversions through gravimetric  $\text{CO}_2$  capture and  $^1\text{H}$  NMR and relate them to refractive indices and viscosity. These data will be presented in subsequent quarterly reports.

In addition to this, refractive index and density are the two key inputs required for obtaining the concentration values from our FT-IR experiments. We will also present the results from the density measurements of the six silyl-amines in the next section.

### **Viscosity**

The viscosity of each compound was measured using a Rheosys Merlin II Viscometer, located in our laboratory. The results for both the molecular and the ionic liquids were presented in the seventh quarterly report.

### **Refractive Index**

The refractive indices for both the molecular and ionic liquid forms were measured using a Reichert Arias 500 Abbe-style refractometer, connected to a circulated cooling bath with glycol as the heat transfer fluid, enabling measurements from 0°C to 75°C. The refractometer is a semi-automatic design which eliminates the need for users to interpret the shadowline intercept, resulting in an accuracy of  $\pm 0.0001$  regardless of user. This will prove important for establishing refractive index as a measure of conversion once the relationship between the two is established.

The refractive index difference between the molecular liquid and the ionic liquid samples is approximately 0.02 for a specific structure at a fixed temperature. The trends in refractive index from a molecular liquid to a fully converted ionic liquid can be linear or can follow a mixing rule such as Lorentz-Lorenz rule. Of all the mixing rules applied to predicting the refractive index of a binary mixture, the Lorentz-Lorenz volumetric mixing rule has shown to be the most accurate for a broad range of liquids and temperatures. The Lorentz-Lorenz mixing rule applied to a binary mixture is,

$$\frac{n_{12}^2 - 1}{n_{12}^2 + 2} = \phi_1 \frac{n_1^2 - 1}{n_1^2 + 2} + \phi_2 \frac{n_2^2 - 1}{n_2^2 + 2} \quad (4)$$

where  $n_{12}$  is the refractive index of the mixture,  $n_i$  is the refractive index of the pure species, and  $\Phi_i$  corresponds to the volume fraction of that species,

$$\phi_1 = \frac{x_1 v_1}{\sum_i x_i v_i} \quad (5)$$

where  $x$  is the mole fraction and  $v$  is the molar volume of component  $i$ .

Carballo<sup>1</sup> and coworkers released an extensive study that examined the refractive index of binary mixtures of ionic liquids and organic solvents, and used the information to determine the validity of the Lorentz-Lorenz mixing rule for determining composition from the refractive index of the mixture. They studied two ionic liquids and five organic solvents having a broad range of refractive indices, molar volumes, and dielectric constants. The conclusion from the paper was that the Lorentz-Lorenz mixing worked extremely well for predicting the composition; in most cases the error from the mixing rule prediction was within the experimental error of their composition assays. In the worst case, the error of the mixing rule approximation was less than  $\pm 5\%$  of the experimentally determined value.

New experiments, where we will compare the actual conversion and refractive indices will validate of Lorentz-Lorenz mixing rules for the reactive systems such as the RevILs systems.

---

1 M.A. Iglesias-Otero, J. Troncoso, E Carballo, *The Journal of Chemical Thermodynamics* Volume 40, Issue 6, June 2008, Pages 949-956

## **Density**

The density measurements were performed using an Anton Paar DMA 38 density meter capable of measurements from 15°C to 40°C with a precision of  $\pm 0.001$  g/mL. This style of densitometer is a vibrating tube densitometer; containing a “U-shaped” tube that is vibrated at its natural frequency. The densitometer records measurements when a stable density is observed over a 15 second period.

### **5- Scrubber Process Design**

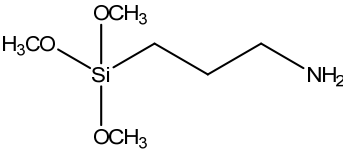
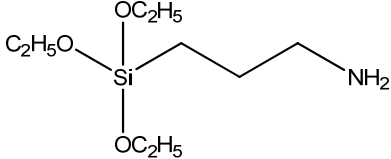
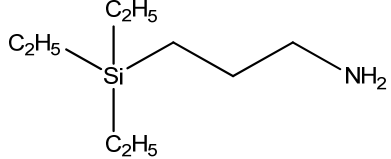
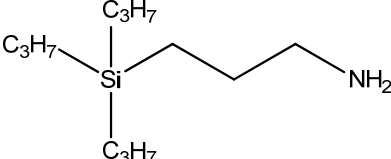
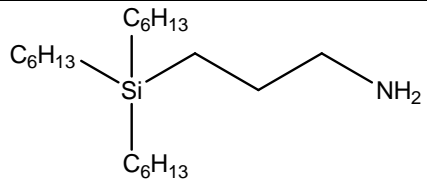
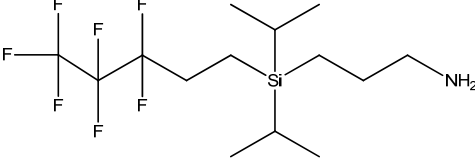
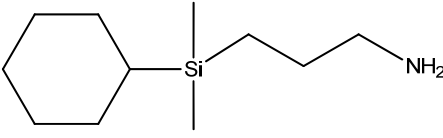
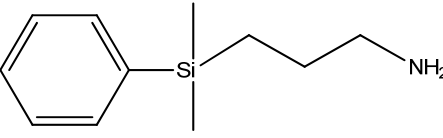
An ASPEN simulation to treat a *model coal-fired power plant flue gas stream has been developed and validation with existing literature data is underway*. Initially, the model will be used to evaluate targets for our CO<sub>2</sub> capture agents to meet the goal of 90% CO<sub>2</sub> capture with no more than a 30% increase in cost. We are using the monoethanolamine (MEA) process as a basis for comparison, and are altering the operating conditions to give us targets for the development of one component reversible ionic liquids. The parameters we seek to optimize are the enthalpy of capture and release, the capture and release temperatures, CO<sub>2</sub> capacities of the solvent, and viscosity of the solvent. The data acquired in the laboratory for the custom-made reversible ionic liquids will be put into the model and evaluated as it is collected, giving us real-time analysis of the economic viability and performance of our solvents. This information will be used to direct the modifications to molecular structure in order for us to meet the goals set forth by DOE and our previous models.

Additional design issues that we plan to consider in the future are the effects of the presence of SO<sub>2</sub>, NO<sub>2</sub>, and carryover gypsum particles from the scrubber in the gas. We believe that our reversible ionic liquids will also absorb SO<sub>2</sub>, but the thermodynamics and kinetics have not yet been investigated. We suspect that the NO<sub>2</sub> will not affect the process as proposed, but need to verify this. The surface of gypsum particles is ionic, so these will probably adsorb small amounts of the ionic liquid, but it is likely that this is reversible with temperature. All these issues will be considered and verified by experiment as we move forward.

## **b. Results and Discussion**

### ***1- Synthesis and Characterization of Custom Reversible ILs***

In this quarter, we have completed the characterization of the (3-aminopropyl) diisopropyl(1H,1H,2H,2H-perfluoropentyl)silane (FSA). In addition, we synthesized two new molecular liquids, (3-aminopropyl) cyclohexyldimethylsilane (CHDMSA) and (3-aminopropyl) phenyldimethylsilane (PDMSA). Our goal was to introduce steric effects into the nitrogen containing molecular liquids to reduce the viscosity of the resulting ionic liquids formed upon reaction with CO<sub>2</sub>. Overall, we have now prepared eight silyl-amine molecular liquids which are listed in Table 1. Synthesis routes for these compounds are discussed in the approach section. <sup>1</sup>H and <sup>13</sup>C NMR characterization of CHDMSA molecular precursor was performed and is reported below. PDMSA has been synthesized and we are currently working on its separation and purification. Complete characterization and analysis of both the molecular liquid and the ionic liquid of these compounds will be presented in the next report.

Compound	Molecular liquid	Structure	Acronym
1	(3-aminopropyl) trimethoxysilane		TMSA
2	(3-aminopropyl) triethoxysilane		TESA
3	(3-aminopropyl) triethylsilane		TEtSA
4	(3-aminopropyl) tripropylsilane		TPSA
5	(3-aminopropyl) trihexylsilane		THSA
6	(3-aminopropyl) diisopropyl(1H,1H,2H,2H-perfluoropentyl)silane		FSA
7	(3-aminopropyl) cyclohexyldimethylsilane		CHDMSA
8	(3-aminopropyl) phenyldimethylsilane		PDMSA

**Table 1: Molecular Liquid Library for Silyl-Amine based CO<sub>2</sub> capture solvents**

**Compound 6. (3-aminopropyl) diisopropyl(1H,1H,2H,2H-perfluoropentyl)silane (FSA).**

NMR Data:

FSA Molecular Liquid <sup>1</sup>H: 2.68(t,2); 2.03(m(pent),2); 1.44(p,2); 1.013(s,16); 0.79(m,2);  
0.58(m,2)

FSA Molecular Liquid <sup>13</sup>C: 45.9, 28.0, 25.9(trip), 18.1, 11.0, 6.4, -1.0

Elemental Analysis:

FSA Molecular Liquid:           Expected: C(45.52), H(7.09), N(3.79)

  Actual: C(45.29), H(7.12), N(3.84)

FSA Ionic Liquid:               Expected: C(44.49), H(6.69), N(3.58)

  Actual: C(44.42), H(6.69), N(3.58)

Distillation Temperature: 100-120°C

Infrared Spectra:

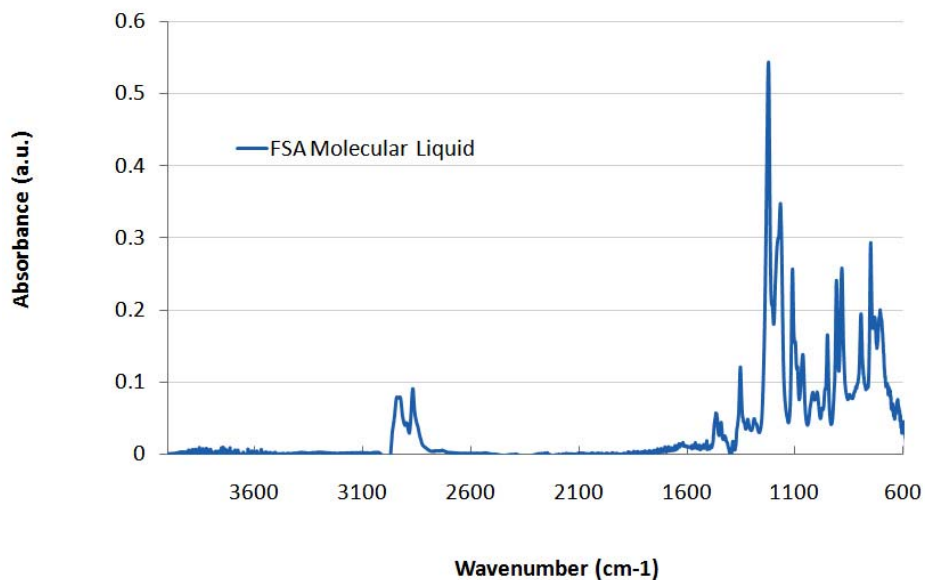


**Figure 3: Infra-red spectra of the FSA molecular liquid and ionic liquid**

DSC Thermogram:

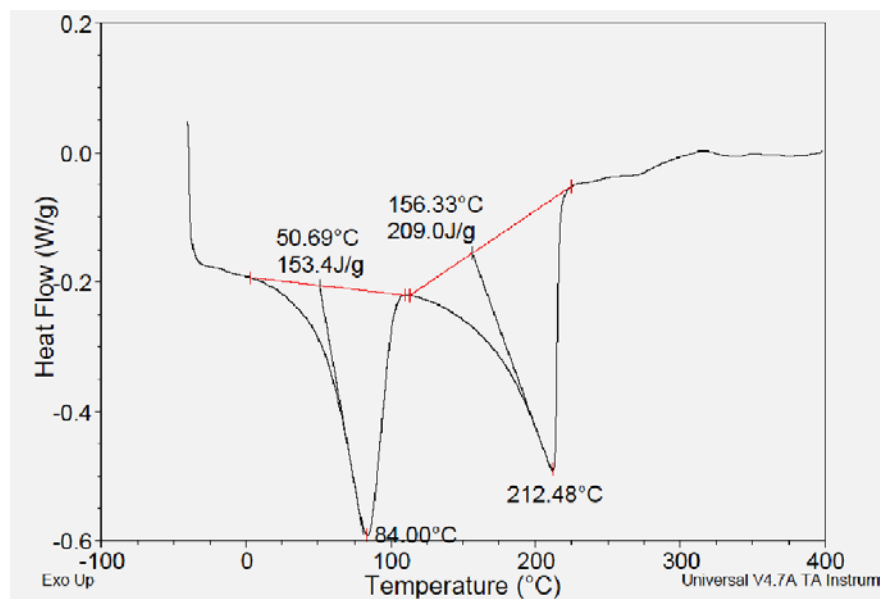


**Figure 4: DSC thermogram of FSA ionic liquid showing reversal reaction and molecular liquid vaporization**

## Compound 7. (3-aminopropyl) cyclohexyldimethylsilane (CHDMSA)

### NMR Data:

CHDMSA Molecular Liquid  $^1\text{H}$ : 2.61 (t,2); 1.66 (s(br), 3); 1.63 (s(br),1); 1.60(s (br), 1); 1.37 (pentet, 2); 1.16 (s (br), 5); .05(t (br), 2); 0.55 (triplet of triplets, 1); 0.42 (mult, 2); -0.12 (s, 6)

CHDMSA Molecular Liquid  $^{13}\text{C}$ : 45.77, 28.36, 28.11, 27.46, 26.99, 25.28, 10.50, -5.39

## 2- Thermodynamics of CO<sub>2</sub> Capture

We have studied the thermodynamics for three alkyl substituted silyl-amines: TEtSA, TPSA, THSA (compounds 3, 4, and 5 in Table1) to determine the effects of the chain length of the substituent groups. Differential Scanning Calorimetry (DSC) was used on preformed ionic liquids to determine the enthalpy required for regenerating the molecular liquid back from the ionic liquid ( $\Delta H_{\text{regeneration}}$ ) and the temperature at which the reversion is initiated ( $T_{\text{rev}}$ ). These two quantities will be extremely useful in designing the scrubber for the CO<sub>2</sub> capture process. DSC thermograms of the three alkyl substituted silyl-amines are shown in figure 5(a), 5(b), and 5(c), respectively. The first event in TPSA and THSA thermograms and the second event for TEtSA represent the reversion of ionic liquid to molecular liquid and CO<sub>2</sub>. The last event in the thermograms for all three compounds is the vaporization of the molecular liquid. The additional (first) event at 22°C in TEtSA thermograms is the melting of the ionic liquid.

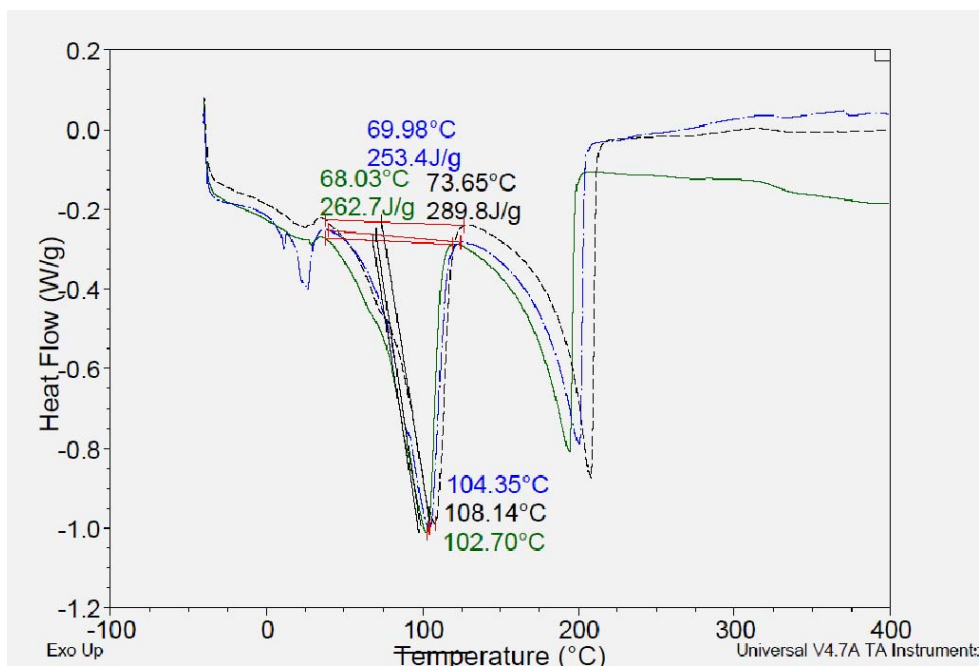


Figure 5(a): DSC runs on three different samples of TEtSA ionic liquid. Blue (dash-dot): sample 1, Green (solid): sample 2, Black (dashed): sample 2. The reversion temperature and regeneration enthalpies have been reported in respective colors.

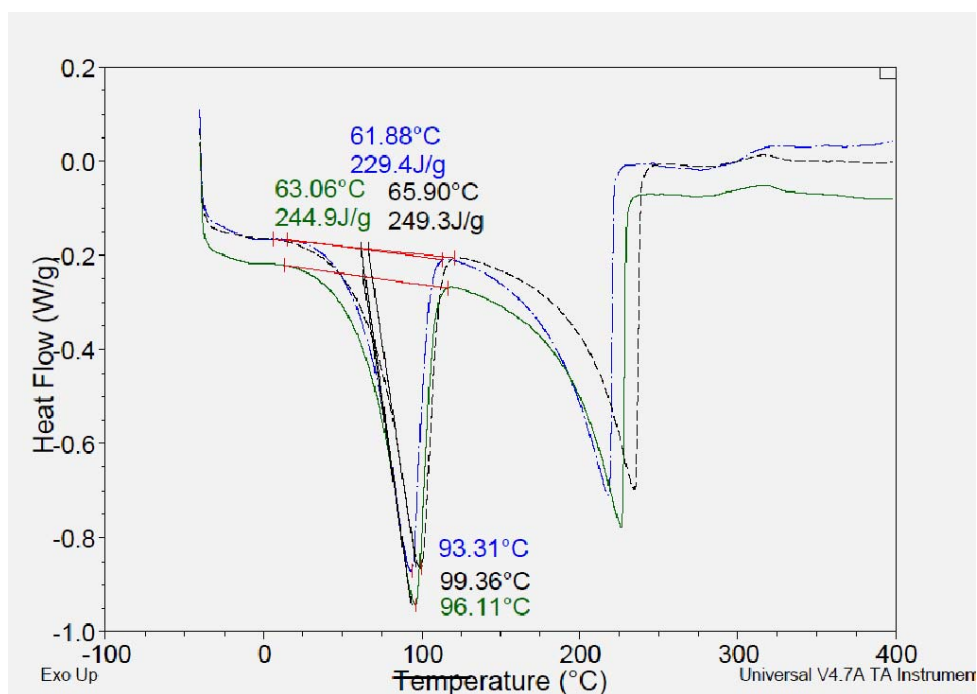
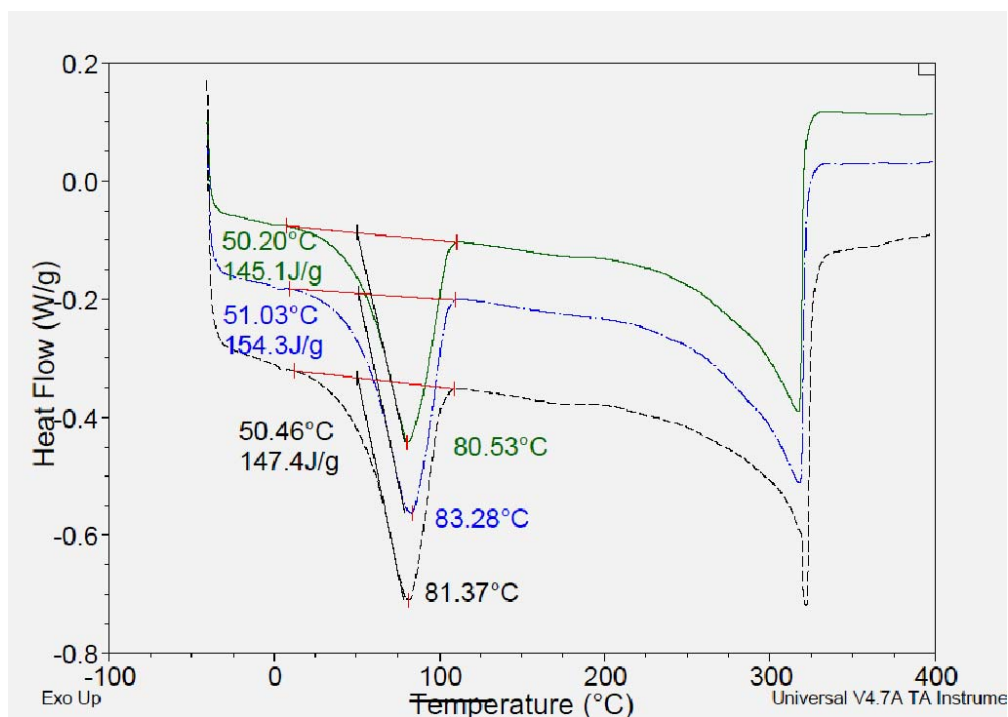


Figure 5(b): DSC runs on three different samples of TPSA ionic liquid. Blue (dash-dot): sample 1, Green (solid): sample 2, Black (dashed): sample 2. The reversion temperature and regeneration enthalpies have been reported in respective colors.



**Figure 5(c): DSC runs on three different samples of THSA ionic liquid. Blue (dash-dot): sample 1, Green (solid): sample 2, Black (dashed): sample 2. The reversion temperature and regeneration enthalpies have been reported in respective colors.**

For each compound, DSC was run in triplicate (on different batches of ionic liquids) and the thermograms for each sample are shown in these figures by green, black, and blue. The  $\Delta H_{\text{regeneration}}$  and  $T_{\text{rev}}$  calculated for each DSC run has also been reported alongside in the same color as the thermogram. For example, the green line in Figure 5(a), depicts the DSC thermogram of the first sample of TEtSA with  $\Delta H_{\text{regeneration}}$  of 262.7 J/g and  $T_{\text{rev}}$  of 68.03°C.

The regeneration enthalpy  $\Delta H_{\text{regeneration}}$  is calculated by integrating the heat flow during reversion with respect to time while  $T_{\text{rev}}$  is the onset temperature of the event found from the intersection of two tangents drawn at the beginning and the bottom of the initial curve. Prior to working with ionic liquids, DSC measurements for enthalpy and onset point were validated by measuring the temperatures and enthalpies associated with the melting and boiling of water. The

melting and boiling enthalpies were found to be within 4% of the literature values, while less than 2% deviation was found for temperatures.

There is a vertical shift in some of the replicate measurements (especially for THSA) which is attributed to difference in the weight of the DSC pans in different runs. These shifts however, do not affect our two quantities of interest  $\Delta H_{\text{regeneration}}$  and  $T_{\text{rev}}$ .

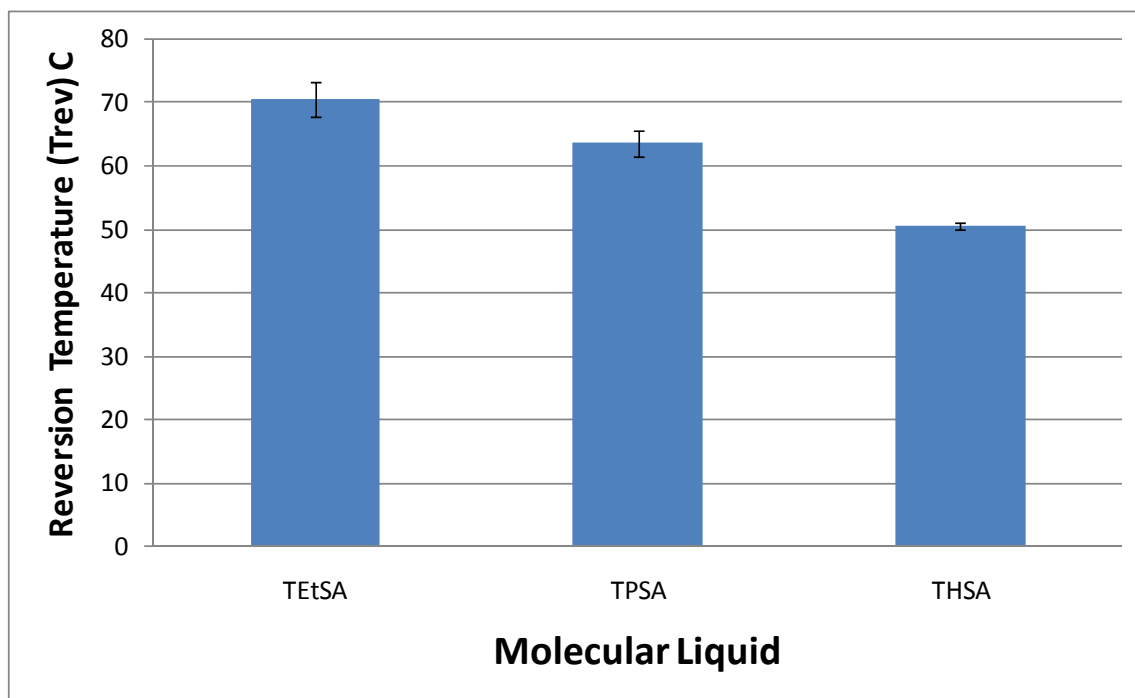
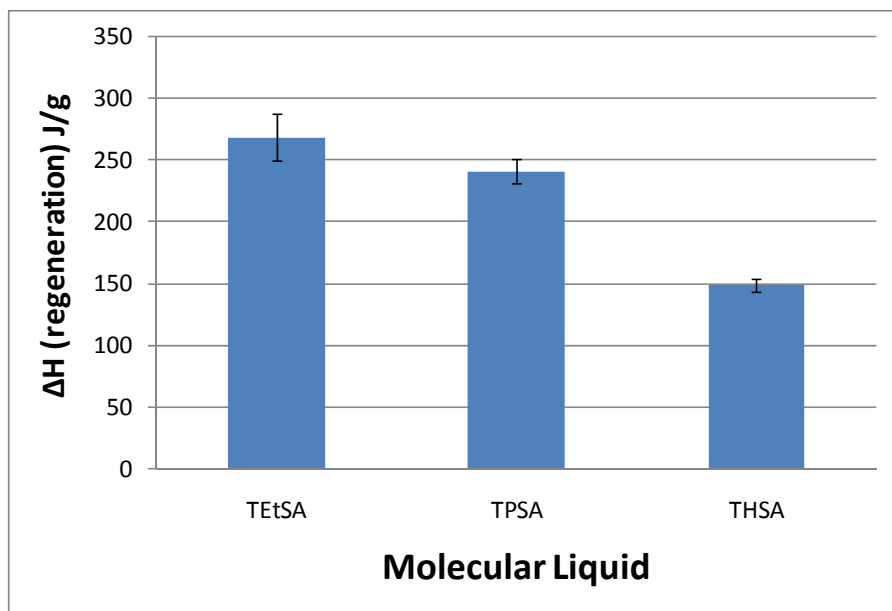


**Figure 6: Reversion temperature of ionic liquids of alkyl-substituted silyl-amines**

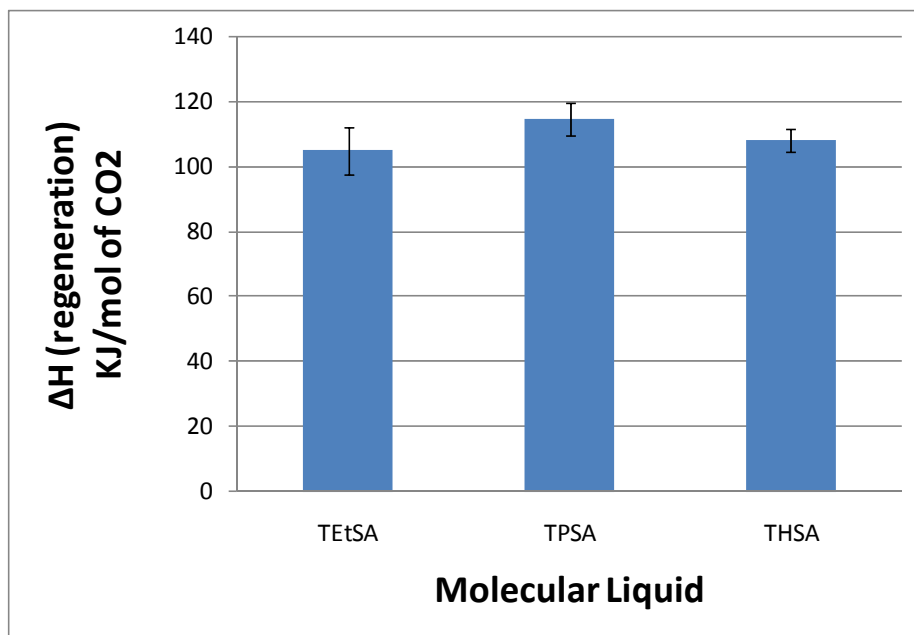
We have compiled the data for reversion temperature  $T_{rev}$  for our silyl-amines in Figure 6. Error bars in the figure indicate the experimental variability during the triplicate runs. The average reversion temperature decreases as we increase the size (chain length) of our substituent groups, from 70.6°C for tri-ethyl substituted silyl-amine to 50.6°C for tri-hexyl substituted silyl-amine.

Figure 7(a) shows the average regeneration enthalpies for the three compounds in J/g which, similar to  $T_{rev}$ , decreases with the increasing substituent size. However, this change is mainly attributed to the increasing molecular weight of these compounds. For all three compounds, the reaction mechanism remains the same: an amine reacting with  $CO_2$  to form ammonium and carbamate ion pair. Hence the enthalpies calculated in KJ per mole of  $CO_2$  captured through chemisorption (considering maximum possible stoichiometric quantities), should be similar to one another. This is shown in Figure 7(b) where the values of average  $\Delta H_{regeneration}$  (in KJ/mol of  $CO_2$ ) are almost similar for the three compounds (the differences in values lie within the range of experimental variability/error bars).

We are currently calculating the K values of these compounds at different temperature conditions to be reported in future reports.



**Figure 7(a):** Enthalpy of regeneration  $\Delta H_{\text{regeneration}}$  in J/g of ionic liquid for alkyl-substituted silyl-amines



**Figure 7(b):** Enthalpy of regeneration  $\Delta H_{\text{regeneration}}$  in KJ/mol of CO<sub>2</sub> for alkyl-substituted silyl-amines

### 3- CO<sub>2</sub> Capture Capacities

#### Overall Capacity:

The combined physisorption (at 1bar) and chemisorption capacity was calculated as the net weight gained by bubbling CO<sub>2</sub> at 1 bar through the molecular precursor at room temperature. The results from the triplicate measurements (with the respective experimental variability) are shown in Figure 8. The overall capacity decreases from TEtSA (0.61 moles CO<sub>2</sub> /moles molecular liquid) to TPSA (0.55 moles CO<sub>2</sub> /moles molecular liquid) and then increases for THSA (0.61 moles CO<sub>2</sub> /moles molecular liquid). This is a result of two simultaneously occurring phenomena with increasing size of the substituent: increasing physisorption and decreasing chemisorption. As shown in Figure 6, the reversion temperature  $T_{rev}$  of these compounds decreases from 70.5°C for TEtSA to 50.5°C for THSA. Therefore, at room temperature (25°C), THSA will be closer to reversion than TPSA, which in turn will be closer than TEtSA. As a result, the room temperature chemisorption would be lower for THSA than TEtSA. This is also evident from Figures 5(a) – 5(c), where the slope of the DSC reversion thermograms at room temperature becomes steeper as we go from TEtSA to THSA.

On the other hand (as will be discussed in greater detail later in the section), bulkier substituent groups provide greater void space and hence greater physisorption. Therefore, the amount of physically captured CO<sub>2</sub> increases from TEtSA and THSA. The opposite trends in chemisorption (room temperature) and physisorption (1bar) result in a parabolic trend in the overall CO<sub>2</sub> capture capacity.

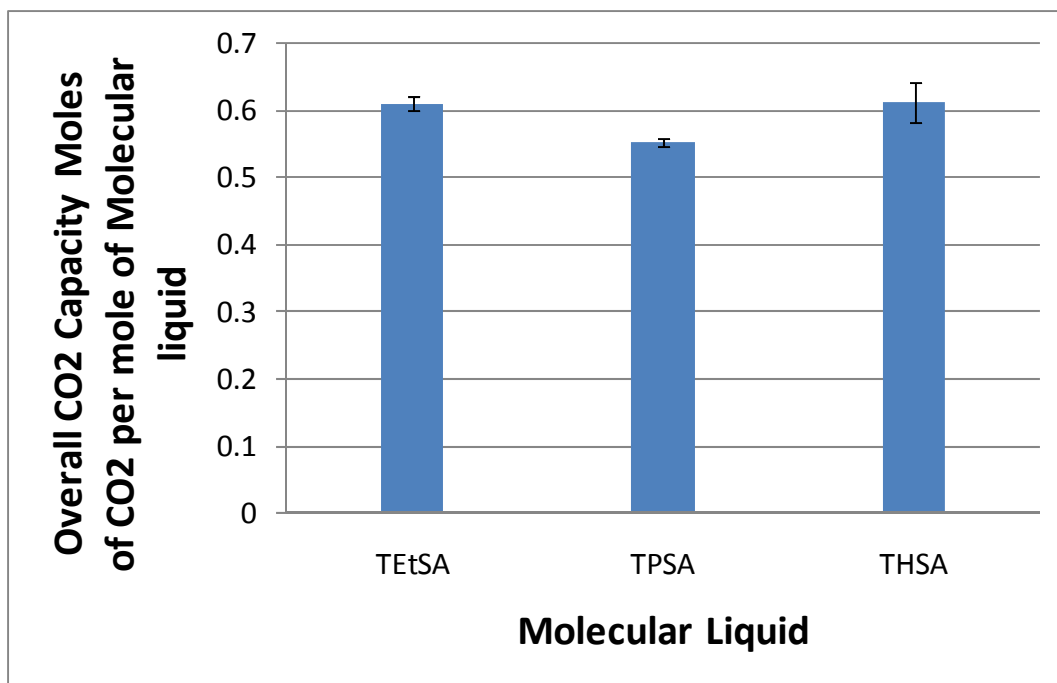


**Figure 8: Overall CO<sub>2</sub> capture capacities found using gravimetric technique for alkyl-substituted silyl-amines**

In Figures 9(a) - 9(c) we have shown TGA thermograms of our ionic liquids. As mentioned in the approach section, TGA experiments were run in parallel with the DSC experiments with the same heating profile to allow for simultaneous analysis of the reverse reaction. The TGA thermograms are shown with solid green lines and are compared with the respective DSC thermograms shown with the dashed blue lines. Corresponding changes in the two thermograms can be seen at the end of the reversal reaction. In TGA thermograms, the weight loss stops at 90-95% of the original weight. The remaining weight is that of the empty pan in which the ionic liquid sample was placed. This merely shifts the graph and does not have any effect on the analysis.

There is a "kink" in the TGA thermogram that depicts two separate processes, i.e. the reverse reaction of ionic liquid to the left and the molecular liquid vaporization to the right. To

de-convolute the two events we plot the derivative of the TGA thermogram, also known as the DTGA. The corresponding DTGA curves are plotted in red with dash-dot lines. The two separate humps in DTGA clearly show the two events in de-convoluted manner. However, the minimum between the two humps does not reach the zero value, thus indicating a slight overlap in the two events, i.e. small amount of molecular liquid vaporization takes place during the reverse reaction as well. This small amount results in slight over-prediction of the CO<sub>2</sub> capture capacity. However, this error will be consistent across the three compounds.

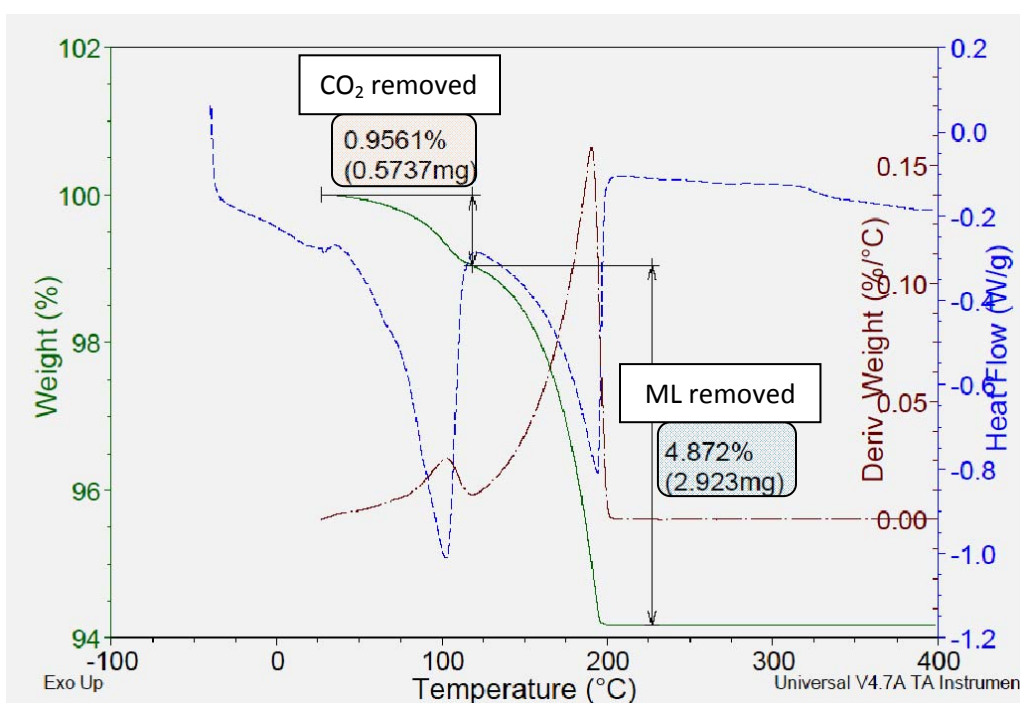


**Figure 9(a): TGA (green, solid) of TETSA compared with its DTGA (red, dot-dash) and DSC (blue, dash). 0.5737mg of CO<sub>2</sub> was released while 2.923mg of molecular liquid was lost through evaporation.**

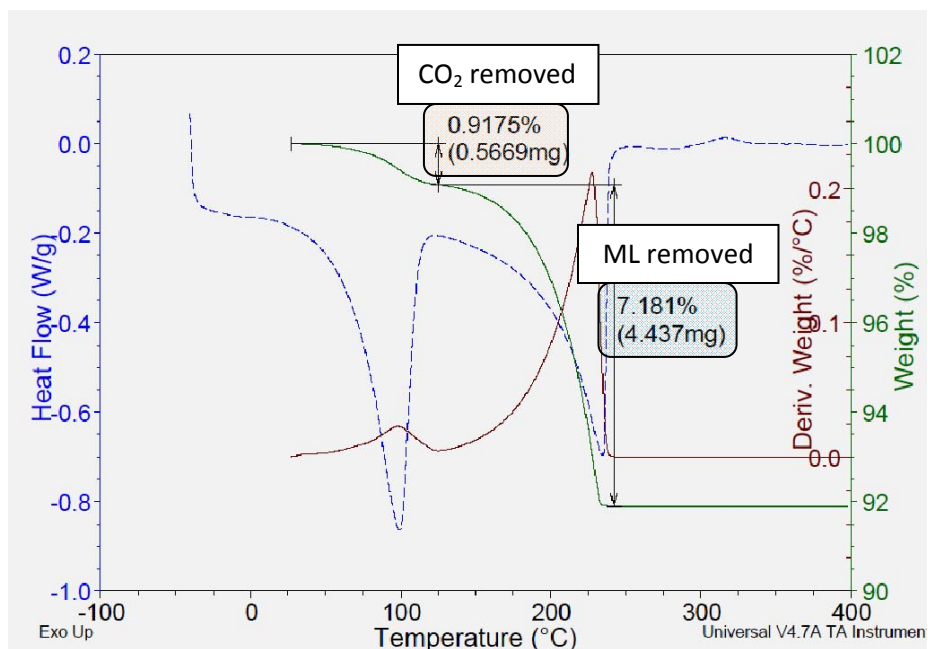


**Figure 9(b): TGA (green, solid) of TPSA compared with its DTGA (red, dot-dash) and DSC (blue, dash). 0.5669mg of CO<sub>2</sub> was released while 4.437mg of molecular liquid was lost through evaporation.**

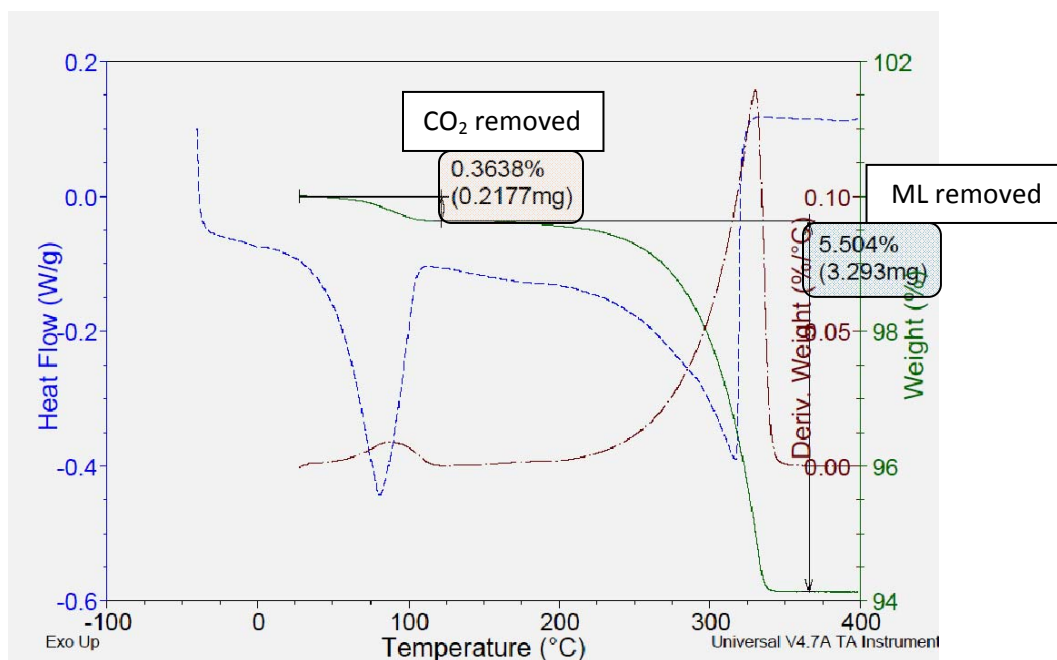


**Figure 9(c): TGA (green, solid) of THSA compared with its DTGA (red, dot-dash) and DSC (blue, dash). 0.2177mg of CO<sub>2</sub> was released while 3.293mg of molecular liquid was lost through evaporation.**

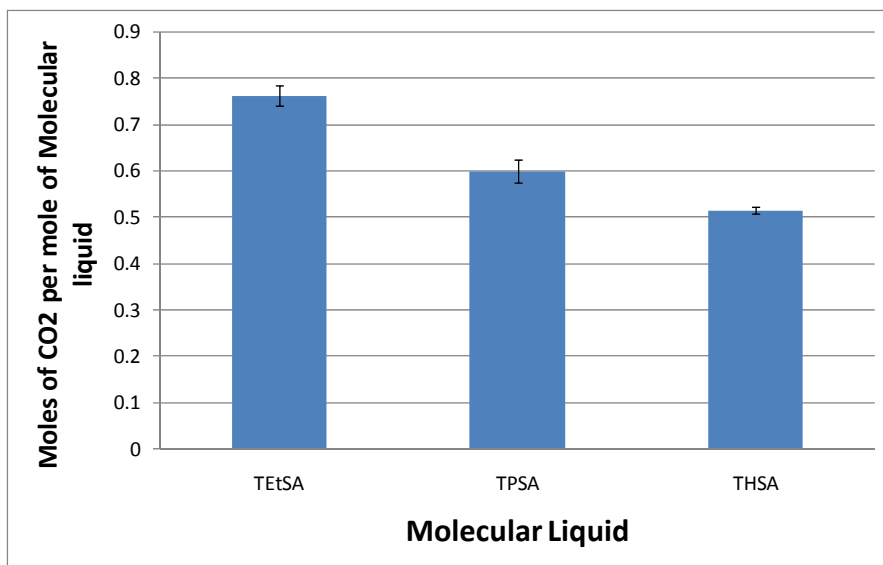


**Figure 10: TGA analysis for ionic liquids of alkyl-substituted silyl-amines.**

For brevity we have shown here only a single TGA thermogram for each compound, but the TGA measurements were taken in triplicate and the results are summarized in Figure 10. The capacities shown in this figure are a sum of chemisorption, physisorption of CO<sub>2</sub> in air, and over prediction due to molecular liquid evaporation. The linear trend in the CO<sub>2</sub> capture capacity from TGA (Figure 10) is quite different from the parabolic trend in the capacity measured by simple gravimetric technique (Figure 8) due to the following reason.

For TGA experiments the preformed ionic liquid samples were exposed to air, which has significantly lower partial pressure of CO<sub>2</sub> than 1 bar. This reduces the amount of physically captured CO<sub>2</sub>. However, physisorption is an equilibrium phenomena and the time required for CO<sub>2</sub> to diffuse out of the ionic liquid and reach equilibrium depends on the viscosity of the ionic liquid. As reported in the 7<sup>th</sup> quarter report, at room temperature, the viscosity of TETSA ionic liquid is almost twice as high as that of THSA. Therefore, THSA will lose CO<sub>2</sub> much faster than TETSA due to the faster CO<sub>2</sub> diffusion through the ionic liquid. Comparison of Figures 8 and 10

shows that THSA loses a significant amount of physically absorbed CO<sub>2</sub>, while for TEtSA the loss of CO<sub>2</sub> is very small. Therefore the parabolic trend changes to the linear one. The higher values of capture capacities from TGA technique as compared to simple gravimetric technique are not surprising as the latter over-predicts due to the vaporization of the molecular liquid.

The other important detail in Figure 10 is that the CO<sub>2</sub> capacity for THSA is barely above the stoichiometric chemisorption limit (0.5 moles per mole of molecular liquid). This value also includes small amounts of physisorbed CO<sub>2</sub> and overprediction due to molecular liquid evaporation. This suggests that for THSA at the room temperature, the amount of chemically absorbed CO<sub>2</sub> is less than the stoichiometric limit of 0.5. This is again in line with the parabolic trend suggested by Figure 8.

To summarize our TGA experiments illustrate two important pieces of information

- There is some molecular liquid evaporation during the reverse reaction
- CO<sub>2</sub> Room temperature chemisorption for THSA is less than the stoichiometric chemisorption limit.

### **Physisorption Capacity:**

The physical absorption capacities of the ionic liquid forms of the six one-component reversible ionic liquids (TMSA, TESA, TEtSA, TPSA, THSA, and FSA, compounds 1-6 in Table 1) were investigated using the reflectance infrared spectroscopic technique. The physical absorption of CO<sub>2</sub> is more attractive than the chemical absorption because of the low thermal requirement of regeneration, where the enthalpy of dissolution for physical absorption is a fraction of the enthalpy of reaction for the chemical absorption. Additionally, when combined

with the chemical absorption, the physical absorption increases the total capture capacity of the solvent thereby increasing the efficiency of the absorption process.

The CO<sub>2</sub> mole fraction ( $x_{\text{CO}_2}$ ) in the ionic liquids TMSA, TESA, and FSA at 35°C is given as a function of CO<sub>2</sub> pressure (bar), Figure 11.

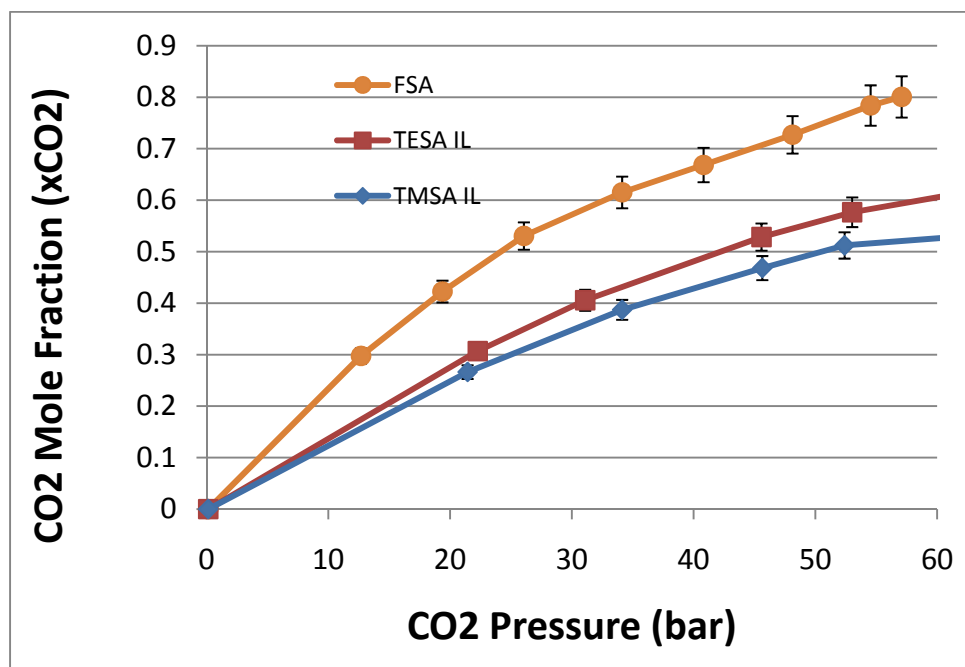


**Figure 11: The solubility of CO<sub>2</sub> in the ionic liquid form of TMSA, TESA, and TMSA as a function of CO<sub>2</sub> pressure (bar) at 35°C.**

It is evident from Figure 11 that the fluorinated material has superior CO<sub>2</sub> solubility to that of the alkoxy- substituted materials. In fact, the FSA compound was identified and synthesized in order to determine the effect of fluorination on physical absorption capacities in the reversible ionic liquids. CO<sub>2</sub> is well known to be fluoro-philic, and fluorinated materials have been shown to exhibit high CO<sub>2</sub> solubility<sup>2,3,4</sup>.

<sup>2</sup> J. Liu, D. Li, H. S. Byun, M. A. McHugh, *Fluid Phase Equilibria* Volume 267, Issue 1, 15 May 2008, Pages 39-46;

The CO<sub>2</sub> mole fraction ( $x_{\text{CO}_2}$ ) in the alkyl- substituted ionic liquids TEtSA, TPSA, and THSA at 35°C is given as a function of CO<sub>2</sub> pressure (bar), Figure 12.

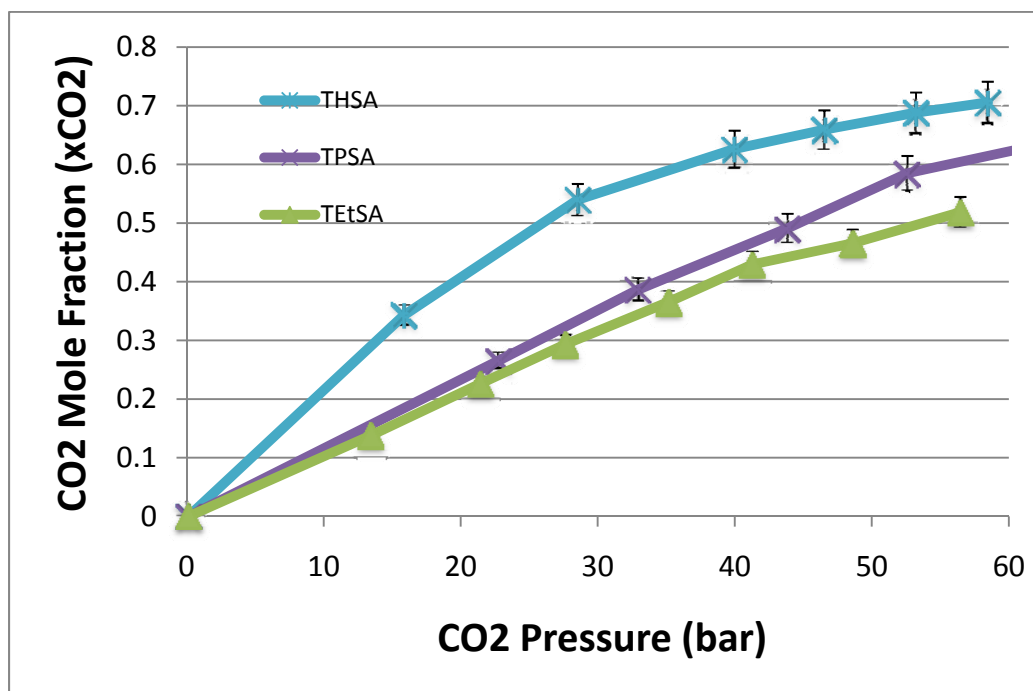


**Figure 12: The solubility of CO<sub>2</sub> in the ionic liquid form of TEtSA, TPSA, and THSA as a function of CO<sub>2</sub> pressure (bar) at 35°C.**

Figure 12 shows that the solubility of CO<sub>2</sub> in the THSA ionic liquid is much higher at a given pressure than the solubility for either TEtSA or TPSA. Additionally, the mole fraction of CO<sub>2</sub> in the ionic liquid is very similar for the TESA/TMSA and TEtSA/TPSA materials; while the THSA and FSA materials exhibit considerably higher capacities. The data indicate that the equilibrium solubility increases with the increasing bulkiness of the ionic liquid. Prof. Brennecke at Notre Dame first postulated that the solubility of CO<sub>2</sub> in ionic liquids is directly related to the void volume of the ionic liquids.<sup>8</sup>

<sup>3</sup> A.J. Mesiano, R.M. Enick, E.J. Beckman, A.J. Russell, *Fluid Phase Equilibria* 178 (2001) 169–177;

<sup>4</sup> T.P. DiNoia, M.A. McHugh, *Macromolecules* 30 (1997) 7511–7515;

The void volume ( $V_V$ ) of the ionic liquid is the “empty” space between the molecules, and is found by subtracting the theoretical van der Waals volume ( $V_{vdW}$ ) from the experimentally determined molar volume ( $V_M$ ). The vdW volume is the theoretical volume the molecule occupies assuming the atoms are hard spheres, one of van der Waals postulates in developing the vdW equation of state. In reality, molecules do not behave as strong spheres. It should be noted that the vdW volume of a molecule is not the addition of the vdW volumes of the atoms that constitute the molecule. Another postulate of van der Waals was that the volume of individual atoms overlap when a bond is formed; hence, the vdW volume of a molecule is always less than the sum of vdW volumes of the individual atoms.

Many methods are available to approximate the vdW volume of materials, including simulation software and group contribution methods. A group contribution method developed by Bondi<sup>5</sup> was released nearly 50 years ago, and provides a simple way for determining vdW volumes of complex molecules by adding the contributions of each individual segment. The vdW volume contributions relevant to the materials studied here are provided in Table 2.

The vdW volume of the “Ion Pair” refers to the volume occupied by the carbamate and ammonium ions. Although Bondi’s work did not include values for ion pairs, it was assumed to involve a secondary amine bound to a carboxylic acid plus a primary amine. Although there is likely to be some error in this assumption, the value is consistent for every ionic liquid reported here. The vdW volumes of several ionic liquids were compared between the Bondi contribution method and a molecular model simulation software program, Spartan ’08, and the values were within good agreement (< 5% difference).

---

<sup>5</sup> A. Bondi, *J. Phys. Chem.* 1964, volume 68, pp 441.

Segment	$V_{vdW}$ (cm <sup>3</sup> /mol)
CH <sub>3</sub> -	13.67
-CH <sub>2</sub> -	10.23
>CH-	6.78
CF <sub>3</sub> -	20.49
-CF <sub>2</sub> -	15.73
-O-	5.2
>Si<	6.82
Ion Pair	38.36

**Table 2: The vdW volume contributions presented by Bondi and used in this study.**

Compound	MW <sub>IL</sub> (g/mol)	$\rho_{IL}$ (g/cm <sup>3</sup> )	$V_M$ (cm <sup>3</sup> /mol)	$V_{vdW}$ (cm <sup>3</sup> /mol)	$V_V$ (cm <sup>3</sup> /mol)
TMSA	402	1.126	357	227	130
TESA	486	1.043	466	288	178
TEtSA	390	0.922	423	257	166
TPSA	474	0.912	520	318	202
THSA	727	0.884	822	502	320
FSA	783	1.193	656	395	261

**Table 3: The void volumes of the ionic liquid forms of the reversible ionic liquids.**

The ionic liquid molecular weights ( $MW_{IL}$ , g/mol), densities at 25°C ( $\rho_{IL}$ , g/cm<sup>3</sup>), molar volumes ( $V_M$ , cm<sup>3</sup>/mol), vdW volumes ( $V_{vdW}$ , cm<sup>3</sup>/mol), and void volumes ( $V_V$ , cm<sup>3</sup>/mol) are given in Table 3.

The relationship between void volume and solubility of CO<sub>2</sub> in the six ionic liquids was examined by first calculating the Henry's Law constant ( $H$ ) of CO<sub>2</sub> in the ionic liquids. Henry's Law is a limiting case of vapor-liquid equilibrium, valid for systems at low solubility, stating that the solubility of a gas in equilibrium with a liquid phase is directly proportional to the partial pressure of the gas in the vapor phase,

$$H_{CO_2} = \lim_{x_{CO_2} \rightarrow 0} \left( \frac{P_{CO_2}}{x_{CO_2}} \right) \quad (6)$$

where  $x_{CO_2}$  is the mole fraction of CO<sub>2</sub> in the liquid phase and  $P_{CO_2}$  is the partial pressure of CO<sub>2</sub> in the vapor phase. The detection limit of the reflectance infrared spectroscopic technique precludes the solubility of CO<sub>2</sub> in the ionic liquids at low pressure as a discernable asymmetric CO<sub>2</sub> vibration wasn't observed for pressures < 10 bar. Henry's Law constants were determined by the straight-line fit (through the origin) of the data points for which  $P_{CO_2} < 35$  bar. A plot of  $H$  (bar, at 35°C) versus  $V_V$  (cm<sup>3</sup>/mol) is given in Figure 13. The errors bars for TESA, TEtSA, TPSA, and FSA are all within the data point.

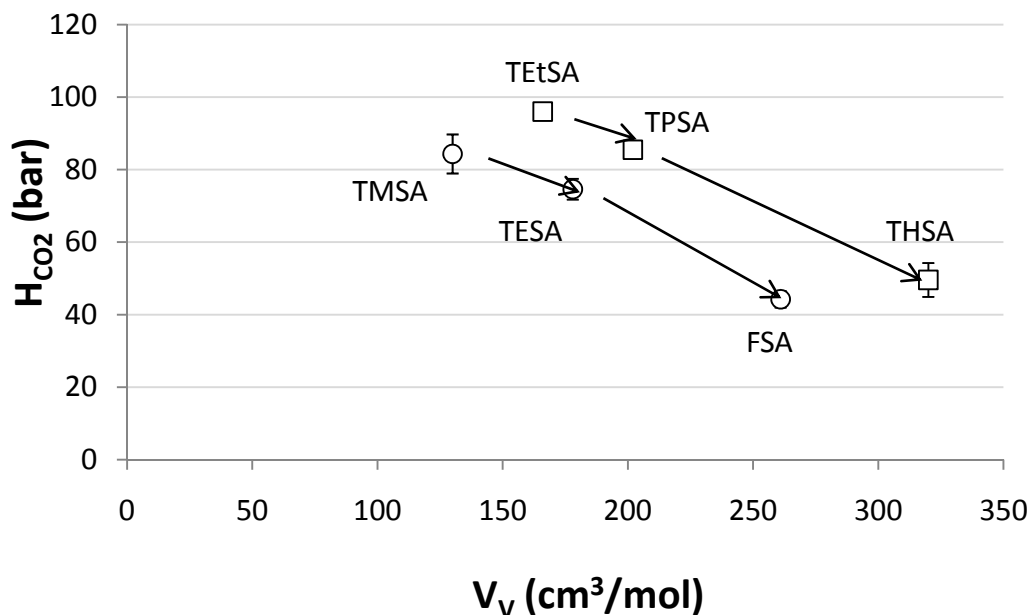


**Figure 13: Plot of Henry's Law constants ( $H$ , bar) versus void volumes ( $V_V$ ,  $\text{cm}^3/\text{mol}$ ) for the ionic liquid forms of TMSA, TESA, TEtSA, TPSA, THSA, and FSA at 35°C.**

Figure 13 shows that  $H_{\text{CO}_2}$  does correlate with  $V_V$  in an apparent linear fashion within a “class” of compounds. The two classes of compounds are (1) trialkyl- substituted materials (represented by the open squares) and (2) the trialkoxy- substituted and fluorinated materials (represented by the open circles). This information is crucial for the design of reversible ionic liquid materials with enhanced physical absorption capacities. The 35°C  $H_{\text{CO}_2}$  values found for the reversible ionic liquids reported here are comparable to the  $H_{\text{CO}_2}$  values of conventional ionic liquids. For example, the  $H_{\text{CO}_2}$  values of the well studied ionic liquid 1-n-butyl-3-methylimidazolium hexafluorophosphate [bmim][PF<sub>6</sub>] were reported to be  $53.4 \pm 0.3$  bar and  $81.3 \pm 0.5$  bar at temperatures of 25°C and 50°C, respectively.

Another important consideration for the design of reversible ionic liquid is how the solubility of physically absorbed CO<sub>2</sub> in the ionic liquid phase changes with temperature. Because our experimental apparatus is only heated and not cooled, temperature control near

room temperature is difficult. Additionally, at high temperatures the ionic liquid is susceptible to reversion back to the molecular liquid which would skew the resulting solubility information. A benefit of the infrared technique for probing CO<sub>2</sub> solubility in the ionic liquids is the ability to monitor the composition of the solvent, where reversion of the ionic liquid is easily detectable and could thus be avoided. Nevertheless, at 50°C and P<sub>CO<sub>2</sub></sub> > 10 bar, the ionic liquids appeared to remain relatively stable and the x<sub>CO<sub>2</sub></sub> information could be collected, shown in Figure for TMSA and TEtSA comparing the solubility data collected at 35°C and 50°C.

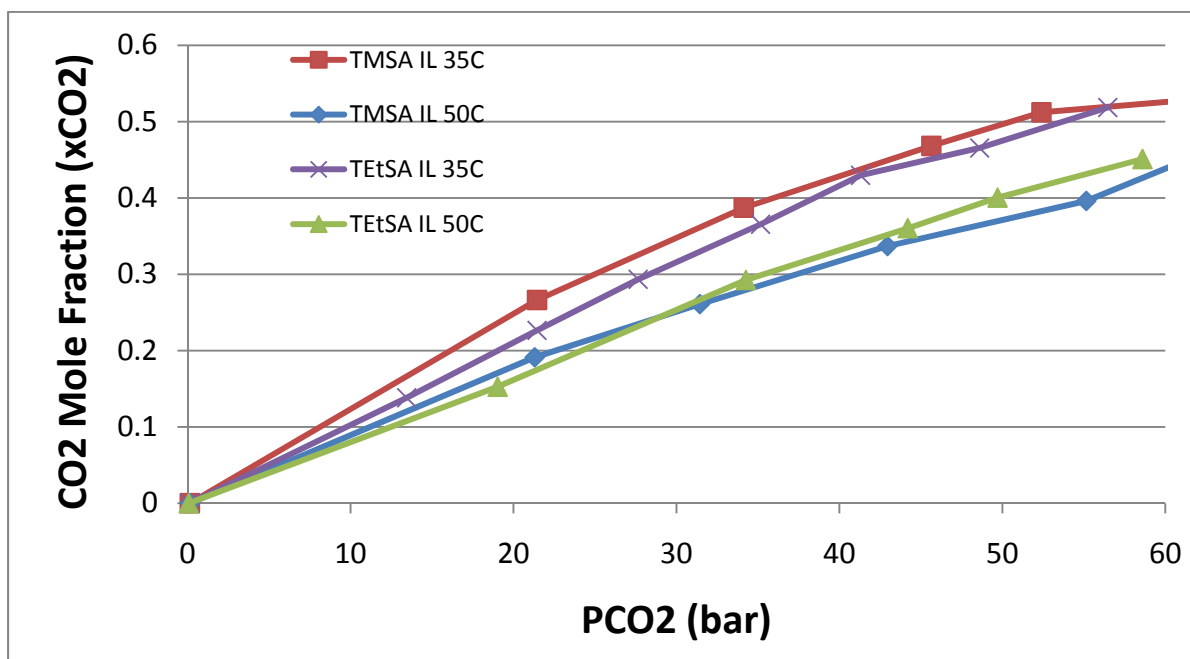


**Figure 14: Plot of CO<sub>2</sub> solubilities (x<sub>CO<sub>2</sub></sub>) as a function of CO<sub>2</sub> pressure (P<sub>CO<sub>2</sub></sub>) for TMSA (open circles) and TEtSA (open squares) at 35°C (solid lines) and 50°C (dashed lines).**

#### **4- Other important Structure-Property relationships: Viscosity, Refractive index, and Density**

##### **Viscosity and refractive index**

In our preliminary experiments, we observed that the refractive indices and viscosities of the ionic liquids were lower when the reaction time was reduced. Figure 15(a) compares the refractive indices and viscosities of TPSA that was allowed to react with CO<sub>2</sub> for short times. The data are not presented with respect to time as the flow rate was not constant for all these experiments and hence the amount of CO<sub>2</sub> reacting with the molecular precursor does not correlate with time. However, as discussed in the approach section, the refractive index of the mixture of ionic and molecular liquid is a very good candidate to monitor the extent of reaction, with higher R.I. representing higher conversion. Although we are currently working towards proving this using <sup>1</sup>H NMR and gravimetric techniques, for this report we are presenting our results assuming this to be true on the basis of various evidences from the literature. The second assumption we shall make is that our mixture is a binary mixture of molecular liquid and ionic liquid and the concentration of free CO<sub>2</sub> in the mixture is very small as compared to the concentration of molecular and ionic liquids. This assumption comes from the greater tendency of CO<sub>2</sub> to enter into the solution and react with the molecular liquid than accumulate through physisorption.

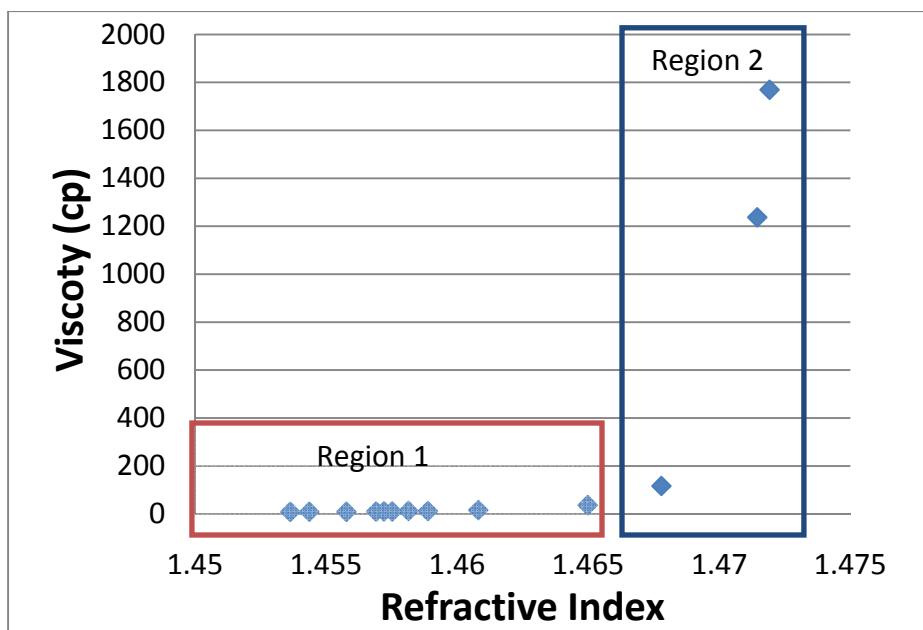


**Figure 15(a).** The viscosity of TPSA as a function of refractive index of the ionic liquid, 25°C.

From Figure 15(a) two regions can be identified: (1) at R.I. values between 1.45 and 1.465, the viscosity is relatively independent of R.I. and hence reaction extent, and (2) at R.I. values higher than 1.465, a highly R.I. (composition) dependent region of viscosity is present. In the low R.I. region, the concentration of ionic liquids is low and the unreacted amine behaves as a solvent and solvates the salt causing dissociation of the ions. To show this we used Lorentz-Lorenz rule discussed in the approach section to convert R.I. to composition. Graph of viscosity as a function of composition is shown in Fig. 15(b). A change in phase composition occurs near R.I. of 1.4675 (ionic liquid composition of 0.6) where the ionic liquid is assumed to change from the solute to the solvent. For the ionic liquid solvent (region 2), small changes in composition (on the order of 1%) can cause drastic changes in viscosity (on the order of 100 cP). The region exhibiting a

strong dependence of viscosity on composition is consistent with published reports that small amounts of co-solvents (or contaminants) result in large changes in the viscosity of ionic liquids<sup>6</sup>

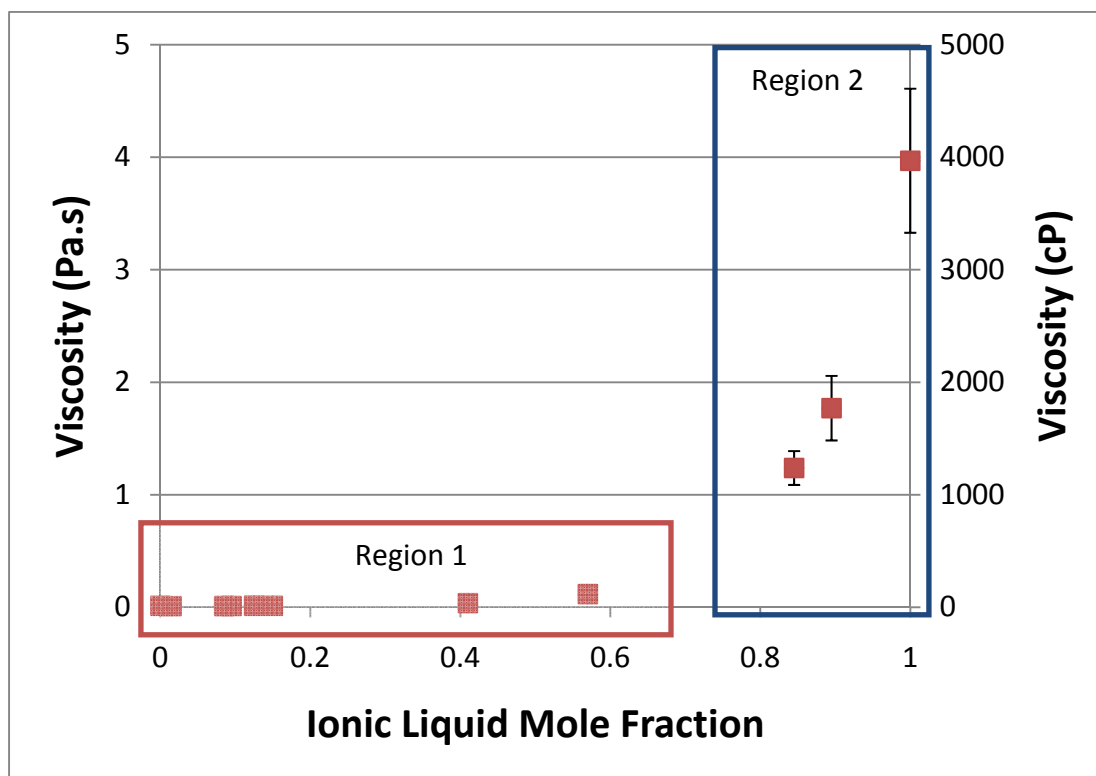


**Figure 15(b): The relatively composition independent region of the viscosity of TPSA as a function of ionic liquid mole fraction, 25°C.**

It is apparent that the high ionic liquid mole fraction region is problematic for processing of the reversible ionic liquids in an absorber configuration. A better examination of the low ionic liquid mole fraction region is offered in Figure 15(b), which expands upon region 1.

Assuming an upper limit of viscosity for good processing solvents to be 100 cP, it is shown that ionic liquid mole fractions up to 0.5 will yield a usable liquid for the application to industrial absorber processes. An ionic liquid mole fraction of 0.5 corresponds to a conversion of the molecular liquid of equal to 67%. This is a considerable conversion to yield a processable

<sup>6</sup> K. R. Seddon, A. Stark, M.J. Torres, *Pure and Applied Chemistry* 2000, volume 72, pp 2275.

fluid; considering the viscosity of the fully formed ionic liquid is near 4000 cP. Although high conversions can be achieved while maintaining low viscosity, as the concentration dependent region of the viscosity plot is approached, small increases in conversion result in drastic increases in viscosity which could be detrimental to the operation of flow processes using reversible ionic liquids as the solvent.

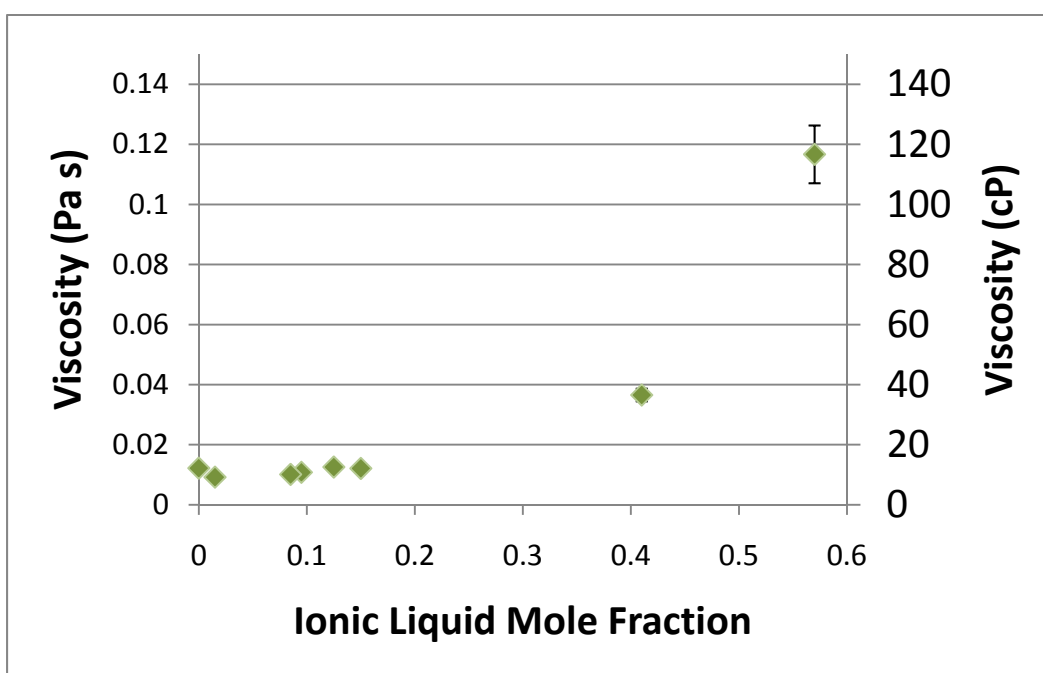


**Figure 15(c). The relatively composition independent region of the viscosity of TPSA as a function of ionic liquid refractive index, 25°C.**

### Density

We have used vibrating type tube densitometer; containing a “U-shaped” tube that is vibrated at its natural frequency. When a sample is placed inside the tube, the frequency of

vibration is dampened proportional to the density of the sample. This is important because the reversible ionic liquids are susceptible to reversion from vibrations, thus forming CO<sub>2</sub> “pockets” in the sample. The densitometer records measurements when a stable density is observed over a 15 second period. The design of the densitometer limited the measurement of the ionic liquids at higher temperatures, except for TEtSA which was successfully analyzed up to 40°C.

The densities of the molecular liquids were measured from 25°C to 40°C, and are shown in Figure 16. The densities of TEtSA, TPSA, and THSA are all very close in value, with substantially higher densities observed for the TMSA, TESA, and FSA molecular liquids. The molecular liquid densities as a function of temperature appear to follow a linear trend, although the temperature range examined is very limited and gross errors could be observed if extrapolations deviate far from this range.

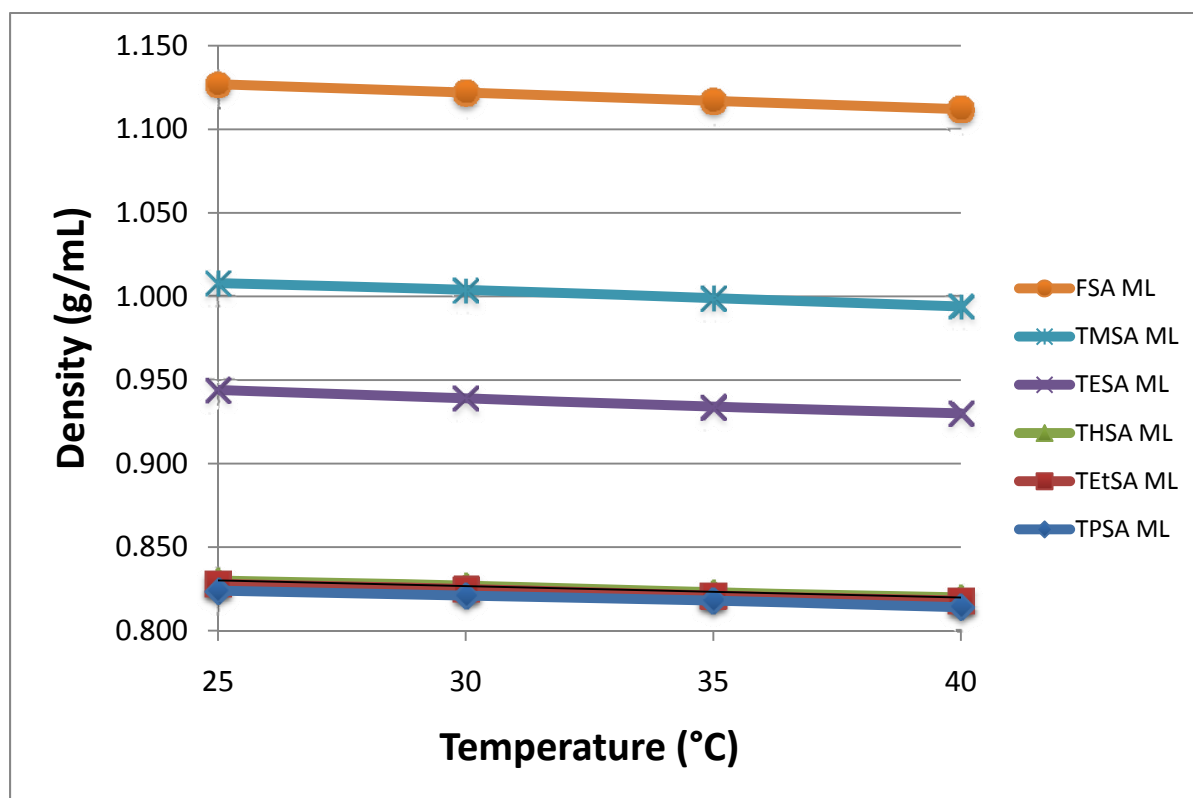


**Figure 16. The one-component molecular liquid densities as a function of temperature.**

The densities of the corresponding ionic liquids are given in Figure . The TETSA ionic liquid sample was the only material that was successfully measured over the entire temperature range, and the two alkoxy- materials were only successfully measured at 25°C. Due to the operation of the densitometer, the vibrations caused pockets of CO<sub>2</sub> to be formed and rise to the interface of the liquid and vibrating tube, causing the density to fluctuate and the densitometer was not able to converge on a density reading.

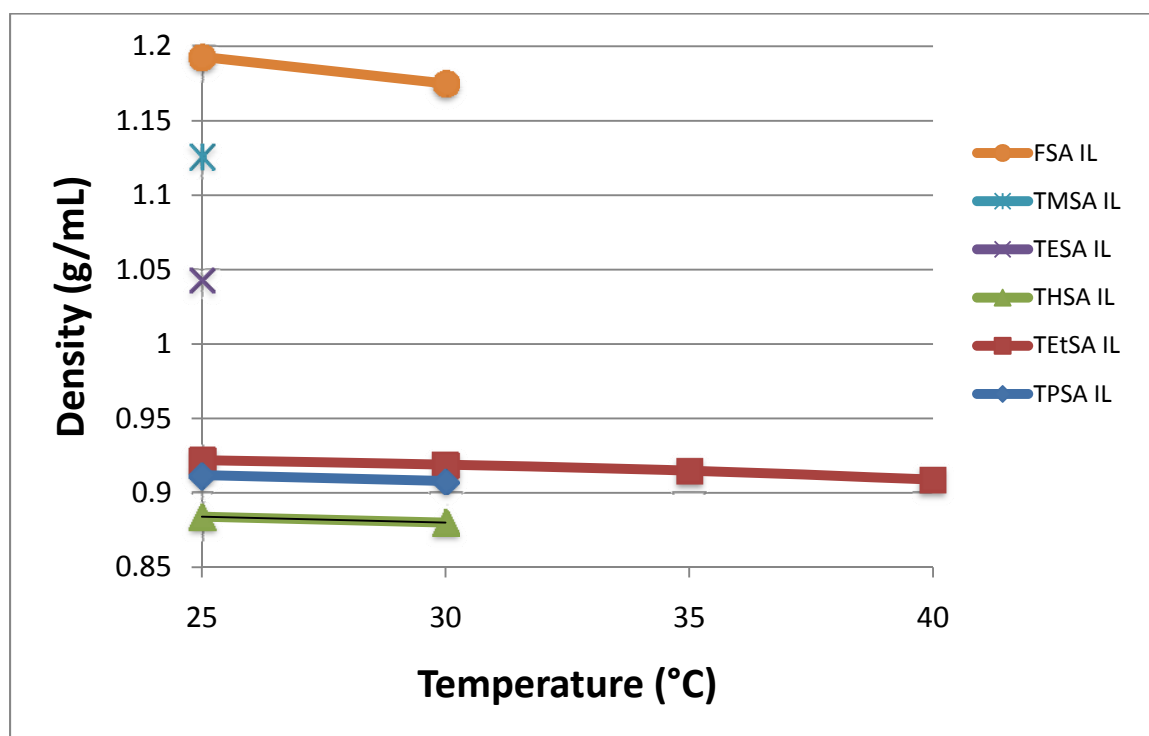


**Figure 17. The one-component ionic liquid densities as a function of temperature.**

The density of the TETSA ionic liquid appears to decrease linearly with respect to temperature. This trend has been observed to be true for conventional room temperature ionic liquids (non-reversible) over broad temperature ranges. All materials exhibit a change in density

of approximately 0.075 g/mL as they are converted from the molecular liquid to ionic liquid, consistent the addition of carbon dioxide that results in the increase in molecular weight.

### c. Conclusion

We continue to make substantial progress towards helping the DOE achieve the goal of 90% CO<sub>2</sub> capture with no more than a 30% increase in cost by 2020. We have made significant accomplishments during the 8<sup>th</sup> Quarter of the project in determining the thermodynamics, CO<sub>2</sub> capture capacities, and viscosities of our silyl-amine based ionic liquids. We have progressed in both the synthesis of new compounds based on the insights gained in the previous quarters and establishing new structure-property relationships that will help us determine the optimum candidates for CO<sub>2</sub> capture solvents.

We have synthesized two new silylated compounds to reduce the viscosity of the ionic liquids (**TASK 2**). We continue to stay ahead of schedule on the thermodynamic analysis (**TASK 4**), and have used several measurement techniques to investigate simultaneously both chemisorption and physisorption in our silylated CO<sub>2</sub> capture solvent candidates. We have achieved several key insights into the structure-property relationships by determining the thermodynamic properties (regeneration enthalpies and reversal temperature) and the overall CO<sub>2</sub> capture capacities of the alkyl substituted silyl-amines, and thus establishing effects of substituent size on these properties. We have also obtained physisorption capacities, Henry's Law constants, and densities for our six ionic liquids, and have established the effects of compound structure on these. (**TASK 5**). In addition, we have conducted preliminary experiments that show controlling the extent of conversion might be the key to obtaining low viscosities, and thus easier processability.

The data being collected are giving insights to modify further the structure of our compounds for enhanced properties for CO<sub>2</sub> capture from fossil fuel-fired power plants. We hypothesize that the silyl-amine reversible ionic liquid candidates are far superior to the one component guanidine reversible ionic liquids (**TASK 3**), and owing to their dual absorption mechanism are proving to be very promising candidates for commercializable CO<sub>2</sub> capture solvents.

## 6. Cost Status

This information is being provided independently by the Grants and Contracts department of Georgia Tech Research Corporation.

### 1. Milestone Status

The milestones listed in the Project Management Plan for Years One and Two were as follows:

<b>ID</b>	<b>Milestone Description</b>	<b>Planned Completion</b>	<b>Verification Method</b>
A	Complete Project Management Plan	10/01/08	PMP approved by DOE COR
B	Complete laboratory synthesis and characterization of one new single-component silyl-amine-based reversible ionic liquid.	6/30/09	laboratory synthesis and characterization of single-component silyl-amine-based reversible ionic liquid.
C	Complete laboratory synthesis and characterization of one new single-component silyl guanidine-based reversible ionic liquid.	9/30/09	Progress Report describing laboratory synthesis and characterization of one new single-component silyl guanidine-based reversible ionic liquid
D	Complete laboratory synthesis and characterization of 2nd new single-component silyl-amine-based reversible	3/30/10:	Progress Report describing synthesis and characterization of 2nd new silyl-amine-based and

	ionic liquid and 2nd new single-component silyl guanidine-based reversible ionic liquid.		guanidine-based reversible ionic liquids
E	Complete synthesis and characterization of single-component Silyl-amine-Based ILs	06/30/10	Synthesis and Characterization results for Silyl-amine-Based ILs documented in Progress Report
F	Complete laboratory measurement of the thermodynamics of formation of one new single-component silyl-amine-based reversible ionic liquid and one new single-component silyl guanidine-based reversible ionic liquid.	9/30/10	Progress Report describing thermodynamics of formation of new single-component silyl-amine-based and single-component silyl guanidine-based reversible ionic liquids
G	1-Component Silyl Guanidine-Based ILs	02/28/11	Synthesis and Characterization results documented in Progress Report
H	Complete laboratory measurements of the rates of formation of one new single-component silyl-amine-based reversible ionic liquid and one new single-component silyl guanidine-based reversible ionic liquid.	3/30/11	Progress Report describing rates of formation of new single-component silyl-amine-based and single-component silyl guanidine-based reversible ionic liquids

In year one, Milestone A was completed on schedule with the approval of the Project Management Plan. Milestone B was completed ahead of schedule, with the complete laboratory synthesis and characterization of four new single-component silyl-amine-based reversible ionic liquids. For Milestone C we proposed to synthesize and characterize a silyl-guanidine based reversible ionic liquid. However, before we achieved this goal, reports came from the Jessop group at Queen's University in Canada showed that in fact that the guanidine based RevILs are

unsuitable for CO<sub>2</sub> capture because high MW compounds are in fact liquids – thereby offering extremely low capacities. We discussed this in our Quarter 6 Report, and are now focusing solely on the silyl-amine-based reversible ionic liquids.

In year two, we have discovered that the silyl-amine-based reversible ionic liquids are much superior to the guanidine-based reversible ionic liquids in terms of both properties and capacity – this was discussed in detail in the progress report for Quarter 6. Therefore we have focused on the silyl-amine-based reversible ionic liquids only. For milestone D, we reported the complete laboratory synthesis and characterization of 3 more (6 total) new single-component silyl-amine-based reversible ionic liquids in the Progress Reports for Quarter 6 & 7, and in this quarter we have synthesized two new compounds (bringing our total tally to 8 compounds) for milestone E. In Quarter 7, we had also reported the viscosities and refractive indices of six compounds both in molecular and ionic forms. Finally, in this quarter, we have gone ahead of our schedule (Milestone F) by measuring the physical absorption capacities of six silyl compounds and other important thermodynamic properties (regeneration enthalpies and reversal temperature) for three alkyl substituted silyl-amines.

As discussed in Quarter 6, progress report we will not continue with Milestone G as it involves the guanidine based solvents. We are currently assessing viable candidates and techniques to pursue Milestone H: Complete laboratory measurements of the rates of formation.

## **2. Summary of Significant Accomplishments**

The significant accomplishments are:

- Synthesize two new silyl-amine based reversible ionic liquids for CO<sub>2</sub> capture.

- Measure CO<sub>2</sub> capture capacities and thermodynamics of three alkyl substituted silyl-amines
- Complete ATR FT-IR studies on six candidates to get information for physical absorption capacities and Henry' Law constants.
- View effects of void volumes on physical absorption.
- Successfully measure densities for molecular and ionic forms of all six candidates.
- Establish correlations between viscosity, refractive index, and conversion
- Identify and synthesize promising target molecules for future synthesis and characterization based on evidence collected during the first 7 Quarters of the project.
- Recent advances have resulted in submittals for publications in scientific journals and presentations at scientific conferences.

### **3. Actual or anticipated problems or delays, and actions taken**

We do not anticipate any future problems or delays.

### **Products produced**

#### **a. Publications**

Vittoria Blasucci, Cerag Dilek, Hillary Huttenhower, Ejae John, Veronica Llopis-Mestre, Pamela Pollet, Charles A. Eckert, and Charles L. Liotta, "One Component, Switchable, Neutral to Ionic Liquid Solvents Derived from Siloxylated Amines," *Chem Comm*, 116-119, 2009.

Vittoria Blasucci, Ryan Hart, Veronica Llopis-Mestre, D. Julia Hahne, Melissa Burlager, Hillary Huttenhower, Reginald Thio, Charles L. Liotta, and Charles A. Eckert, “Single Component, Reversible Ionic Liquids for Energy Applications,” *Fuel*, **89**, 1315–1319, 2010.

Vittoria M. Blasucci, Ryan Hart, Pamela Pollet, Charles L. Liotta, and Charles A. Eckert, “Reversible Ionic Liquids Designed for Facile Separations,” *Fluid Phase Equilibria*, **294**, 1-6, 2010.

## **b. Presentations**

### ***1- Invited papers:***

Charles A. Eckert and Charles L. Liotta, “Reversible Ionic Liquids as Double-Action Solvents for CO<sub>2</sub> Capture,” Annual NETL CO<sub>2</sub> Capture Technology for Existing Plants R&D Meeting, Pittsburgh, PA, September 13, 2010.

Charles A. Eckert and Charles L. Liotta, “Reversible Ionic Liquids as Double-Action Solvents for CO<sub>2</sub> Capture,” Annual NETL CO<sub>2</sub> Capture Technology for Existing Plants R&D Meeting, Pittsburgh, PA, March 24, 2009.

Ryan Hart, Charles L. Liotta and Charles A. Eckert, “Molecular Design of Liquid Sorbents for CO<sub>2</sub> Capture,” Georgia Tech CO<sub>2</sub> Forum, September 2009

Charles A. Eckert, Ryan Hart, Vittoria Blasucci, Pamela Pollet, and Charles L. Liotta, “Smart” Solvents for Extractions and Purifications, Annual AIChE Meeting, Nashville, TN, November,

2009.

Charles A. Eckert and Charles L. Liotta, "Novel Solvents for Sustainable Technology," Basore Distinguished Lecture, Auburn University, January 2010

Charles L. Liotta and Charles A. Eckert, "Solvent Systems for Green and Sustainable Chemical Processes," BASF, Wyandotte, MI, March 18, 2010

Charles L. Liotta and Charles A. Eckert, "Solvent Systems for Green and Sustainable Chemical Processes," Virginia Commonwealth University, Richmond, VA, March 31, 2010

Charles L. Liotta and Charles A. Eckert, "Solvent Systems for Green and Sustainable Chemical Processes," Chemistry Department, U. Texas, Dallas, Wyandotte, TX, April 8, 2010.

Charles A. Eckert, Charles L. Liotta, Pamela Pollet, Ryan Hart, "Provoking Phase Changes for Extractive Separations," AIChE Annual Meeting, Salt Lake City, UT, November, 2010.

***2- Contributed Papers:***

Vittoria Blasucci, Cerag Dilek, Hillary Huttenhower, Ejae John, Veronica Llopis-Mestre, Pamela Pollet, Charles L. Liotta, and Charles A. Eckert "One-Component, Switchable, Neutral to Ionic Liquid Solvents Derived from Siloxylated Amines," 237th National Meeting, ACS, Salt Lake City, UT, March, 2009.

Vittoria Blasucci, Ryan Hart, Cerag Dilek, Hillary Huttenhower, Veronica Llopis-Mestre, Pamela Pollet, Eduardo Vyhmeister, Charles L. Liotta, and Charles A. Eckert, "Reversible Ionic Liquids as Double-Action Solvents for Efficient CO<sub>2</sub> Capture," AIChE Spring National Meeting, Tampa, FL, April 2009

Philip G. Jessop, Michael Cunningham, Charles A. Eckert, and Charles L. Liotta "CO<sub>2</sub> as a Trigger for Switchable Chemistry," International Conference on Carbon Dioxide Utilization, China, May 2009.

Ali Fadhel, Vittoria Blasucci, Cerag Dilek, Ryan Hart, Hillary Huttenhower, Veronica Llopis-Mestre, Pamela Pollet, Eduardo Vyhmeister, Charles A. Eckert, and Charles L. Liotta "Designer Reversible Ionic Liquids for CO<sub>2</sub> Capture," 13th Annual Green Chemistry & Engineering Conference, Washington, DC, June 2009.

Ryan Hart, Vittoria Blasucci, Charles A. Eckert, and Charles L. Liotta, "Development of One-Component Reversible Ionic Liquids for Energy Applications," 2009 Annual AIChE Meeting, Poster, Nashville, TN, November 2009.

Ryan Hart, Pamela Pollet, Dominique J. Hahne, Ejae John, Veronica Llopis-Mestre, Vittoria Blasucci, Hillary Huttenhower, Walter Leitner, Charles A. Eckert, Charles L. Liotta, "A Unique Class of Sustainable Solvents: Reversible Ionic Liquids," ACS Spring Meeting, March 21 – 25, 2010, San Francisco.

Cerag Dilek, Vittoria Blasucci, Ali Fadhel, Kyle Flack, Ryan Hart, Hillary Huttenhower, Kristen Kitagawa, Veronica Llopis-Mestre, Pamela Pollet, Manjusha Verma, Eduardo Vyhmeister, Charles L. Liotta, and Charles A. Eckert, "Reversible Ionic Liquids as Dual Functional Solvents for Post Combustion CO<sub>2</sub> Capture " 6th Chemical Engineering Conference for Collaborative Research in Eastern Mediterranean Countries (EMCC6), March 2010, Antalya-Turkey.

Rani Jha, Ali Fadhel, Vittoria Blasucci, Ryan Hart, Veronica Llopis-Mestre, Pamela Pollet, Charles L. Liotta, Charles A. Eckert, "Designer Reversible Ionic Liquids for CO<sub>2</sub> Capture," Fall National Meeting, ACS, Boston MA, August, 2010.

Ryan Hart, Kyle Flack, Jackson Switzer, Amy Rohan, Manjusha Verma, Charles L. Liotta, and Charles A. Eckert, "The Design of Reversible Ionic Liquids for Post-Combustion CO<sub>2</sub> Recovery," AIChE Annual Meeting, Salt Lake City, November 2010.

Jackson R. Switzer, Amy L. Rohan, Ryan J. Hart, Pamela Pollet, Charles L. Liotta, Charles A. Eckert, "A Spectroscopic Technique for the Decoupled Measurement of Physical and Chemical Absorption in Reactive Solvent Systems," Pittcon, Atlanta, GA, March 13-18, 2011.

Swetha Sivaswamy, Ryan Hart, Kyle Flack, Pamela Pollet, Charles Liotta and Charles Eckert, " Reversible ionic liquids for carbon dioxide capture," ACS Meeting, Anaheim, CA, March 2011

Jackson Switzer, Kyle Flack, Ryan Hart, Amy Rohan, Swetha Sivaswamy, Elizabeth Biddinger, Manish Talreja, Manjusha Verma, Pamela Pollet, Charles Liotta, Charles Eckert, " Design of Dual-Capture CO<sub>2</sub> Solvents using Structure-Property Relationships," 2011 Georgia Tech Research and Innovation Conference (Poster).

Amy Rohan, Ryan Hart, Kyle Flack, Swetha Sivaswamy, Jackson Switzer, Elizabeth Biddinger, Manish Talreja, Pamela Pollet, Charles Liotta and Charles Eckert, " Advance of Reversible Silylamine-Based Ionic Liquids for Post-Combustion CO<sub>2</sub> Capture from Coal-Fired Power Plants," 2011 Georgia Tech Research and Innovation Conference (Poster).

Amy Rohan, Ryan Hart, Kyle Flack, Swetha Sivaswamy, Jackson Switzer, Elizabeth Biddinger, Manish Talreja, Pamela Pollet, Charles Liotta and Charles Eckert, " Use of Reversible Ionic Liquids as Solvents for Post-Combustion Recovery of CO<sub>2</sub> from Coal-Fired Power Plants," AIChE National Meeting, Chicago, IL, March 2011.

### **c. Website**

Webpages have been prepared and posted within the Eckert/Liotta group website

<http://www.chbe.gatech.edu/eckert/projects.html>.

### **d. Intellectual Property**

One invention disclosure based on the work of this project has been filed. It is Eckert, C.A., Liotta, C.L., Huttenhower, H.; Mestre-Llopes, V.; Blasucci, V.; Pollet, P.; "Reversible Ionic Liquids as Double Action Solvents for Efficient CO<sub>2</sub> Capture", Invention disclosure 9/29/2008.

### **e. Education**

A major thrust of this project is the education of our future scientists and engineers who will be working in the environmental area developing sustainable processes. We are pleased to report our contributions in this area:

#### **Personnel/Students Graduated**

Dr. Ryan Adams, (Chemical Engineering, Postdoctoral)

Vittoria Blasucci – PhD in Chemical Engineering, 2009 – Now at ExxonMobil

Hillary Huttenhower – PhD in Chemistry, 2010 – Now at Pratt & Whitney

#### **Personnel/Students Continuing**

Dr. Pamela Pollet (Chemistry, Research Scientist)

Dr. Elizabeth Biddinger, (Chemical Engineering, Postdoctoral)

Dr. Rani Jha, (Chemistry, Postdoctoral)

Dr. Manish Talreja, (Chemical Engineering, Postdoctoral)

Dr. Manjusha Verma, (Chemistry, Postdoctoral)

Olga Dzenis (PhD Candidate, Chemical Engineering)

Ali Fahdel (PhD Candidate, Chemical Engineering)

Kyle Flack (PhD Candidate, Chemistry)

Ryan Hart (PhD Candidate, Chemical Engineering)

Greg Marus (PhD Candidate, Chemical Engineering)

Amy Rohan (PhD Candidate, Chemical Engineering)

Swetha Sivaswamy (PhD Candidate, Chemical Engineering)

Jackson Switzer (PhD Candidate, Chemical Engineering)

Melissa Burlager (Senior, Chemical Engineering)

Paul Nielsen (Senior, Chemical Engineering)

Sean Faltermeier (Senior, Chemical Engineering)

Poomrapee Jewanarom (Sophomore, Chemical Engineering)

### **High School Students**

We have high school science students working in our lab each summer.

The most recent have been A from X High School in Atlanta and B from Y High School in Marietta, GA.

## **f. Industrial Collaboration**

As a result of our work on this project we have generated an industrial collaboration with ConocoPhillips, who have agreed to partner with us for the next three years. This not only provides for facile technology transfer, but gives us enhanced access to real-world problems and opportunities. And of course, it provides a vehicle for future testing and implementation.